ARMY RESEARCH LABORATORY

# The Attenuation of Microwave Radiation by Fog and Rain

By J. D. Pendleton
Stanley Niles
Battlefield Environment Directorate

19941129 070

NOTICES

Disclaimers

The findings in this report are not to be construed as an official Department of the Army position, unless so designated by other authorized documents.

The citation of trade names and names of manufacturers in this report is not to be construed as official Government indorsement or approval of commercial products or services referenced herein.

Destruction Notice

When this document is no longer needed, destroy it by any method that will prevent disclosure of its contents or reconstruction of the document.

REPORT DOCUMENTATION PAGE			Form Approved OMB No. 0704-0188

1. AGENCY USE ONLY (Leave blank)	2. REPORT DATE August 1994	3. REPORT TYPE AND DATES COVERED Final	

4. TITLE AND SUBTITLE

The Attenuation of Microwave
Radiation by Fog and Rain

5. FUNDING NUMBERS

6. AUTHOR(S)

J.D. Pendleton and Stanley Niles

7. PERFORMING ORGANIZATION NAME(S) AND ADDRESS(ES)

U.S. Army Research Laboratory
Battlefield Environment Directorate
ATTN: AMSRL-BE-E
White Sands Missile Range, NM 88002-5501

8. PERFORMING ORGANIZATION REPORT NUMBER

ARL-TR-527

9. SPONSORING/MONITORING AGENCY NAME(S) AND ADDRESS(ES)

U.S. Army Research Laboratory
2800 Powder Mill Road
Adelphi, MD 20783-1145

10. SPONSORING/MONITORING AGENCY REPORT NUMBER

ARL-TR-527

11. SUPPLEMENTARY NOTES

12a. DISTRIBUTION/AVAILABILITY STATEMENT

Approved for public release; distribution is unlimited.

12b. DISTRIBUTION CODE

A

13. ABSTRACT (Maximum 200 words)

In this report, the equations which describe the attenuation of long-wavelength electromagnetic radiation by water fogs and rain are briefly reviewed and explained under the assumption that the aerosol droplets are spherical and that the irradiance of the beam is in the "linear" regime. Calculations of water fog attenuation coefficients are made using the Rayleigh approximation, and an approximate error analysis of this approximation is made by comparing Rayleigh approximation calculations of absorption efficiency with exact Mie theory calculations of extinction efficiency. Numerical integration of the Mie extinction efficiency is used to compute the attenuation coefficient for rain with a Marshall-Palmer drop size distribution for various rain rates and temperatures. These results are compared with those given by a power law relationship with coefficients given by Olsen, Rogers, and Hodge which was used in the Near Millimeter Wave (NMMW) Module of the Electro-Optical Systems Atmospheric Effects Library (EOSAEL).

14. SUBJECT TERMS

microwave, fog, rain, aerosol, droplets, attenuation coefficients, Rayleigh, Mie theory, Olsen, Rogers, and Hodge

15. NUMBER OF PAGES

70

16. PRICE CODE

17. SECURITY CLASSIFICATION OF REPORT	18. SECURITY CLASSIFICATION OF THIS PAGE	19. SECURITY CLASSIFICATION OF ABSTRACT	20. LIMITATION OF ABSTRACT
unclassified	unclassified	unclassified	SAR

Contents

1

Figures

Appendix Figures

Tables

1. Introduction

Explosive missile warheads were used by the U.S. Navy during the Persian Gulf War to generate electromagnetic pulses (EMP) for the purpose of disabling electronic components such as computer chips. The objective of this action was to neutralize communications, command, control, and intelligence (C^3I) systems. Because of the Navy's air attack role, particular emphasis was given to disabling air defense electronic systems.

In this report, equations describing the attenuation of long-wavelength electromagnetic radiation by water fogs and rain are briefly reviewed and explained; the assumption is made that aerosol droplets are spherical and that irradiance of the beam is in the linear regime (i. e., the irradiance is not high enough to produce nonlinear effects such as gas breakdown and explosive vaporization of the droplets).

Calculations of water fog attenuation coefficients are made using the Rayleigh small particle approximation. An error analysis of this approximation is made by comparing Rayleigh approximation calculations of absorption efficiency with exact Mie theory calculations of extinction efficiency. The Rayleigh approximation is appropriate for fog with drop diameters up to 100 μm for frequencies less than 50 GHz. Comparisons are made of Rayleigh absorption efficiencies and Mie extinction efficiencies for rain with water drops up to 5.0 mm; for frequencies above 1 GHz, the use of the Rayleigh approximation is not appropriate. For various rain rates and temperatures, numerical integration of the Mie extinction efficiency is used to compute the attenuation coefficient for rain with a Marshall-Palmer (MP) drop size distribution. These results are compared with those given by a power law relationship with coefficients given by Olsen, Rogers, and Hodge (ORH); this relationship was used in the Near Millimeter Wave (NMMW) Module of the Electro-Optical Systems Atmospheric Effects Library (EOSAEL). The ORH relationship gives very good results at temperatures where the coefficients were determined (from -20 to 20 °C). As temperature increases above 20 °C, the exact Mie calculations deviate increasingly from the results of ORH. The use of the ORH equation is not recommended above 20 °C. The exact Mie computations are recommended; this approach can be performed at any temperature and can be quickly done on a personal computer.

2. Defining and Computing the Attenuation Coefficients With Mie Theory

D.R. Brown [1] provided equations to help compute the attenuation coefficient for clouds, fog, ice fog, and rain. A discussion of issues related to these natural obscurants was given. A more detailed treatment of the theory is given here but only spherical particles will be considered.

The number density (i. e., number per unit volume) of spherical particles with diameters between D_1 and D_2 is given by integration of the size distribution function N with respect to the sphere diameter D in the following equation:

$$\Delta n \ (D_1, D_2) \ = \ \int_{D_1}^{D_2} N \ dD. \tag{1}$$

If $D_1 = 0$ and $D_2 = \infty$, the total number density is obtained. The extinction cross section [2] α_{ext} is usually a function of D and the attenuation coefficient α_{ext} is as follows:

$$\alpha_{ext} \ = \ \int_0^\infty N\sigma_{ext} \ dD. \tag{2}$$

In the absence of multiple scattering, the significance of the attenuation coefficient α_{ext} is the irradiance I of a wave propagating in the z direction is given as a function of z by the following expression:

$$I(z) \ = \ I(z=0) \ e^{(-\alpha_{ext}z)}, \tag{3}$$

where the choice of $z = 0$ is arbitrary. The attenuation coefficient α_{ext} has the unit of (length)$^{-1}$. In engineering literature, an attenuation coefficient α with the units of decibels (dB) per unit length (usually km) is commonly used. The way to express the relation between α and α_{ext} which holds for any unit of length is as follows:

$$\alpha = \left[\frac{10 \ dB}{\ln(10)} \right] \alpha_{ext} \tag{4}$$

$$\approx \left[4.343 \ dB \right] \alpha_{ext}.$$

The reason for introducing α is not always clear. However, recalling that $\exp(-x) = 10^{-x/\ln(10)}$ allows equation (3) to be rewritten with the help of equation (4) as follows:

$$\frac{I(z)}{I(z=0)} = 10^{\frac{-\alpha z}{10 dB}}. \tag{5}$$

Equation (5) is a simple way to determine how many orders of magnitude an electromagnetic wave is attenuated at a particular range z; this is the reason for introducing α. Note that 10 dB = 1 bel (B); the convention is to use dB rather than B.

The power attenuated by a particle, P_{ext}, is equal to the sum of the power scattered by the particle and the power absorbed by the particle. Absorbed power refers to the heat generated in the particle due to Joule heating under irradiation by an electromagnetic wave.

The extinction cross section is defined as follows:

$$\sigma_{ext} = \frac{P_{ext}}{I_{inc}}, \tag{6}$$

where I_{inc} is the irradiance of the incident beam. The extinction efficiency, Q_{ext}, is defined as follows:

$$Q_{ext} = \frac{P_{ext}}{P_{inc}}, \tag{7}$$

where P_{inc} is the power of the incident beam passing through the area of the particle if it is not there. Since the following is true:

$$P_{inc} = I_{inc}\left(\pi\frac{D^2}{4}\right), \tag{8}$$

then

$$\sigma_{ext} = Q_{ext}\left(\pi\frac{D^2}{4}\right) \tag{9}$$

8

and substituting into equation (2) gives the following:

$$\alpha_{ext} = \frac{\pi}{4} \int_0^\infty Q_{ext} \, D^2 N \, dD. \qquad (10)$$

A small particle approximation for Q_{ext} is used for fog, allowing equation (10) to be integrated analytically without specifying a particular particle size distribution. For rain, equation (10) is evaluated by numerically integrating over a particular particle size distribution; Q_{ext} is computed by using the following Mie theory expression: [2]

$$Q_{ext} = \frac{2}{X^2} \sum_{N=1}^\infty (2n+1) \, \mathrm{Re}(a_n + b_n). \qquad (11)$$

The a_n and b_n are referred to as scattering coefficients [2] and X is the Mie size parameter which is defined by the following relation:

$$X = \pi \frac{D}{\lambda}, \qquad (12)$$

where λ is the wavelength of the incident electromagnetic wave in the surrounding medium. Before computing Q_{ext} using either Mie theory or a small particle approximation, it is necessary to obtain $\hat{N}$ the complex refractive index of the sphere's medium relative to the surrounding medium; this is a function of λ. For a harmonic wave with time dependence of $\exp(-i\omega t)$, $\hat{N}$ is written as follows:

$$\hat{N} = \mathrm{Re}(\hat{N}) + i\mathrm{Im}(\hat{N}), \qquad (13)$$

where $\mathrm{Re}(\hat{N})$ and $\mathrm{Im}(\hat{N})$ are both greater than zero. In the appendix, a method for computing $\hat{N}$ for water in the frequency range $1 - 1000$ GHz is discussed; this method is used for both rain and fog.

3. Small Particle (i. e., Rayleigh) Approximation for α_{ext}

In a particle size range where a simple analytical approximation for the extinction efficiency Q_{ext} is known, equation (10) can be analytically integrated to produce an expression for the attenuation coefficient. Bohren and Huffman [2] discuss approximations which hold if spherical particles are small, producing the following result:

$$Q_{abs} = 4X \, Im(Z), \tag{14}$$

where

$$Z = \frac{\hat{N}^2 - 1}{\hat{N}^2 + 2}. \tag{15}$$

According to Bohren and Huffman, [2] equation (14) holds if the following is true:

$$\frac{4}{3} X^3 \, Im(Z) \ll 1. \tag{16}$$

If equation (14) is a good approximation and if the scattering efficiency is much less than the absorption efficiency, then the following is true:

$$Q_{ext} \approx 4X \, Im(Z). \tag{17}$$

Substituting equation (17) into equation (10) produces the following:

$$\alpha_{ext} = \frac{6\pi}{\lambda} \, Im(Z) \int_0^\infty \frac{\pi D^3}{6} \, N \, dD. \tag{18}$$

The mass of water M_w in a given volume of water V_W is as follows:

$$M_w = \rho_w V_w, \tag{19}$$

where ρ_w is the density of the water.

The following relation is also useful:

$$M_w = CV_a, \tag{20}$$

where C is the water content (i. e., water concentration = mass of water per unit volume of air) and V_a is the volume of air.

Setting equation (19) equal to equation (20) and rewriting the result produces the following:

$$\frac{V_w}{V_a} = \frac{C}{\rho_w} \tag{21}$$

and since the following is also true:

$$\frac{V_w}{V_a} = \int_0^\infty \frac{\pi D^3}{6} N \, dD, \tag{22}$$

equation (18) can be written as follows:

$$\alpha_{ext} = \frac{6\pi}{\lambda} Im(Z) \frac{C}{\rho_w}. \tag{23}$$

Since the index of refraction of the air surrounding the water droplets does not differ greatly from vacuum, a reasonable approximation is that $\lambda = C/f$, where $C = 2.9979 \times 10^{10}$ cm/s is the speed of light in vacuum and f is the frequency. This approximation allows equation (23) to be rewritten as follows:

$$\alpha_{ext} = \frac{6\pi f}{C} Im(Z) \frac{C}{\rho_w}. \tag{24}$$

In the Rayleigh approximation, α_{ext} is proportional to C, the concentration of water in the atmosphere. Initial conclusions indicate that α_{ext} is also proportional to the frequency f; however, Z is a function of frequency, so α_{ext} is not exactly proportional to f.

12

4. Computer Calculations of α for Fog Using the Rayleigh Approximation

Liebe et al. [3] have given Rayleigh calculations of α for water for $f = 0 - 1000$ GHz at $T = 20$ °C with $C = 1$ g/m³. Liebe's published results can be used as a benchmark to verify the accuracy of attenuation calculations performed in this investigation.

For computer calculations, it is necessary to rewrite equations (23) and (24) in nondimensional form. If α_{ext} has units of (km)$^{-1}$, λ has units of cm, f has units of GHz, C has units of g/m³, and p_w has units of g/cm³, then the nondimensional expressions of equations (23) and (24) appropriate for computer programming or use with an electronic calculator are as follows:

$$\alpha'_{ext} = \frac{0.6\pi}{\lambda'} \operatorname{Im}(Z) \frac{C'}{\rho'_w} \tag{25}$$

$$\alpha'_{ext} = \frac{0.6\pi f'}{29.979} \operatorname{Im}(Z) \frac{C'}{\rho'_w} \tag{26}$$

where

$$\alpha' = \alpha_{ext}/(km)^{-1}$$
$$\lambda' = \lambda/cm$$
$$f' = f/GHz$$
$$C' = C/[g/m^3]$$
$$\rho'_w = \rho_w/[g/cm^3].$$

If α has the units of dB/km, equation (4) may be rewritten as follows:

$$\alpha' = \frac{10}{\ln(10)} \alpha'_{ext}, \tag{27}$$

where $\alpha' = \alpha/[dB/km]$.

A computer code based on equations (26) and (27) was written to see if the results presented in the work of Liebe et al. [3] for α as a function of f could

be reproduced. It was necessary to compute the complex index of refraction of water as a function of frequency. This was done using the double-Debye formulation given by Liebe et al. [3] A review of the double-Debye formulation is given in appendix A.

The results of these calculations of α as a function of f are compared in table 1 with those given by Liebe et al. [3] Pruppacher and Klett [4] state that the water content of most fogs is less than 0.1 g/m^3. Therefore, a fog with C = 1 g/m^3 is a very heavy fog; values of α in most fogs would be an order of magnitude smaller than reported for C = 1 g/m^3. A water content of C = 1 g/m^3 represents a worst case. α is also given for C = 0.1 g/m^3, a more typical case.

Table 1. Attenuation coefficient α as a function of frequency in the small particle approximation with $\rho_w = 1$ g/cm^3

f/GHz	Liebe et al. For C = 1 g/m^3 α/[dB/km]	This work For C = 1 g/m^3 α/[dB/km]	This work For C = 0.1 g/m^3 α/[dB/km]
300	15.0	15.801	1.5801
400	20.3	20.641	2.0641
500	25	25.197	2.5197
800	38	36.830	3.6830
1000	43	42.598	4.2598

Liebe et al. [3] also shows curves of α as a function of frequency for f = 20 – 1000 GHz for temperatures in a range from -20 to +20 °C. These curves are reproduced in figure 1. Figure 2 indicates the same curves for f = 1 – 350 GHz, showing more detail in the lower frequencies. At frequencies greater than 200 GHz, attenuation caused by water fog and clouds increases with temperature. At frequencies less than 50 Hz, the attenuation decreases with temperature (i. e., the effect of uniformly heating water fog and clouds at frequencies less than 50 GHz increases the propagation). Figure 3 shows detailed results for α at microwave frequencies 0.1 – 8 GHz.
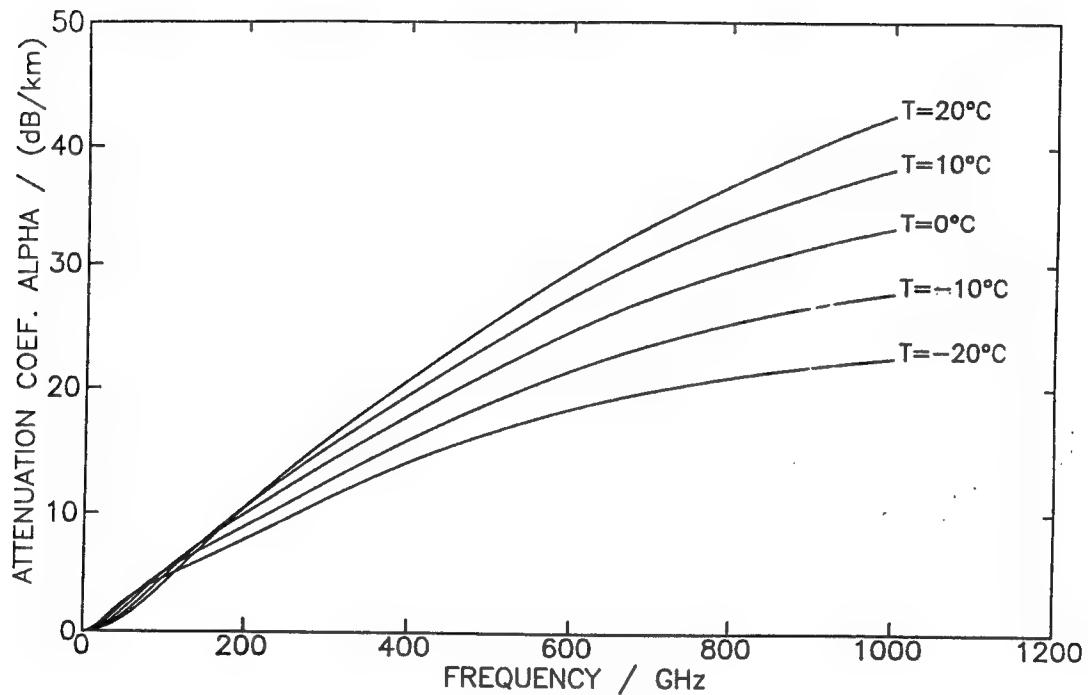
Figure 1. Attenuation coefficient of water fog versus frequency for f = 20 — 1000 GHz; computed using the Rayleigh approximation for water concentration of 1 g/m³ with T = -20 to 20 °C.
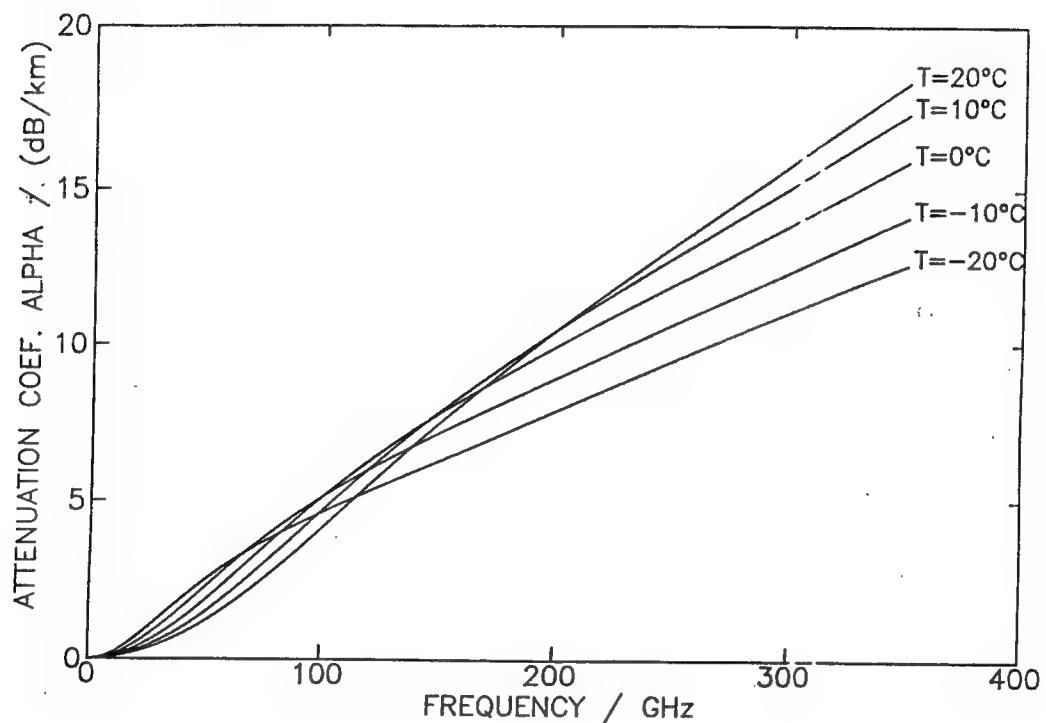
Figure 2. Attenuation coefficient of water fog versus frequency for f = 1 — 350 GHz; computed using the Rayleigh approximation for water concentration of 1 g/m^3 with T= -20 to 20 °C.

16

5. Sample Calculations of Intensity Attenuation Using the Attenuation Coefficient Curves

Once the attenuation coefficient α is determined for a fog, cloud, or rain, equation (5) can be used to determine the attenuation of intensity at a given range.

For example, if $T = 20$ °C and $f = 400$ GHz, figure 1 shows that a heavy fog with $C = 1$ g/m^3 has an attenuation coefficient α approximately equal to 20 dB/km. Since α is proportional to the water concentration in the fog, $C = 0.8$ g/m^3; the resulting value of α is [(20 dB/km)/(1 g/m^3)](0.8 g/m^3) (i. e., $\alpha = 16$ dB/km).

At a range of 5 km, $\alpha z = 80$ dB; equation (5) then gives the result that $I(z)/I(z=0) = 10^{-8}$ so that the electromagnetic wave would be attenuated by eight orders of magnitude, a significant amount. For a more typical fog under the same conditions with $C = 0.1$ g/m^3, $\alpha z = 10$ dB and $I(z)/I(z=0) = 10^{-1}$; the electromagnetic wave would be attenuated by only one order of magnitude. The attenuation of a fog is extremely dependent on range and water content.

The attenuation of microwaves with frequencies less than 10 GHz is much less than for higher frequencies. If $T = 20$ °C, $C = 1$ g/m^3, and $f = 8$ GHz, figure 3 shows that α is approximately equal to 0.04 dB/km. If $C = 0.8$ g/m^3, then $\alpha = 0.032$ dB/km; and at a range of 5 km, $\alpha z = 0.16$ dB. Equation (5) then gives the result that $I(z)/I(z=0) = 10^{-0.016} = 0.964$. The beam is attenuated by less than 4 percent compared to eight orders of magnitude for a beam with $f = 400$ GHz.

For the more typical fog with $C = 0.1$ g/m^3, $\alpha z = 0.020$ dB, and $I(z)/I(z=0) = 10^{-0.0020} = 0.995$; the attenuation is less than 1 percent at a range of 5 km. At shorter ranges, the attenuation is negligible.
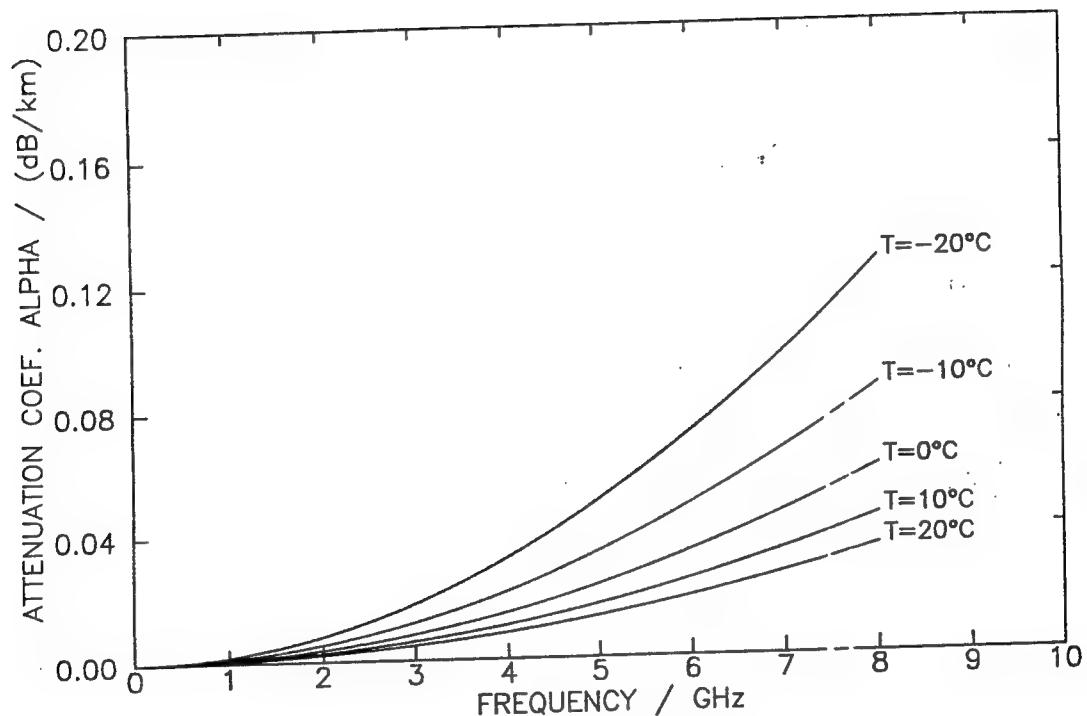
Figure 3. Attenuation coefficient of water fog versus frequency for f = 0.1 — 8 GHz; computed using the Rayleigh approximation for water concentration of 1 g/m³ with T = -20 to 20 °C.

6. Analysis of Rayleigh Attenuation Coefficient Calculations

The Rayleigh approximation used for these calculations is of great interest because it allows the attenuation coefficient to be calculated for fog or a cloud without specifying a particular size distribution. The Rayleigh results are independent of the particular size distribution. The only requirement is that the particles be small.

Accuracy of Rayleigh attenuation coefficient calculations can be determined for a particular size distribution by numerically integrating equation (10); a more general qualitative approach is to compare the Rayleigh absorption efficiency with the Mie extinction efficiency over a size range for a given temperature and frequency. This is done in the next series of figures for water droplets with diameters of 0.5 – 100 μm at temperatures of -20 and 20 °C. Figures 4 through 13 are for frequencies of 10, 50, 300, 600, and 1000 GHz. Before analyzing the results, equation (15) is rewritten as follows:

$$X \approx \pi D \frac{f}{c}$$

$$\approx (1.04793)(10^{-5}) \left(\frac{D}{\mu m} \right) \left(\frac{f}{GHz} \right). \tag{28}$$

Equation (28) shows that an increase in frequency corresponds to an increase in the Mie particle size parameter, and X increases to about 1 when $f = 1000$ GHz for $D = 100$ μm.

Figures 4 and 5 show close agreement between the Rayleigh and Mie results at 10 GHz with more extinction predicted for the lower temperature. Figures 6 and 7 indicate essentially the same results for 50 GHz, but figures 8 through 13 show that the Rayleigh results increase in error as the frequency increases up to 1000 GHz, at which point $X \approx 1$ when $D = 100$ μm. However, the error at 1000 GHz in this size range is still less than an order of magnitude. For fog with maximum diameters of 100 μm, Rayleigh theory is exact at microwave frequencies less than 10 GHz, within a few percent at 50 GHz, and gives better than order of magnitude predictions up to 1000 GHz. There is increasing error with the Rayleigh approximation as frequency and particle size increase.

The Mie extinction efficiency decreases with increasing temperature for $f = 10$ and 50 GHz but increases with temperature for $f = 300$, 600, and 1000 GHz. This agrees with the Rayleigh result that attenuation decreases with increasing temperature for microwaves propagating through water fog.

TEMPERATURE = −20 °C
FREQUENCY = 10 GHz

—— MIE EXTINCTION
------ RAYLEIGH ABSORPTION
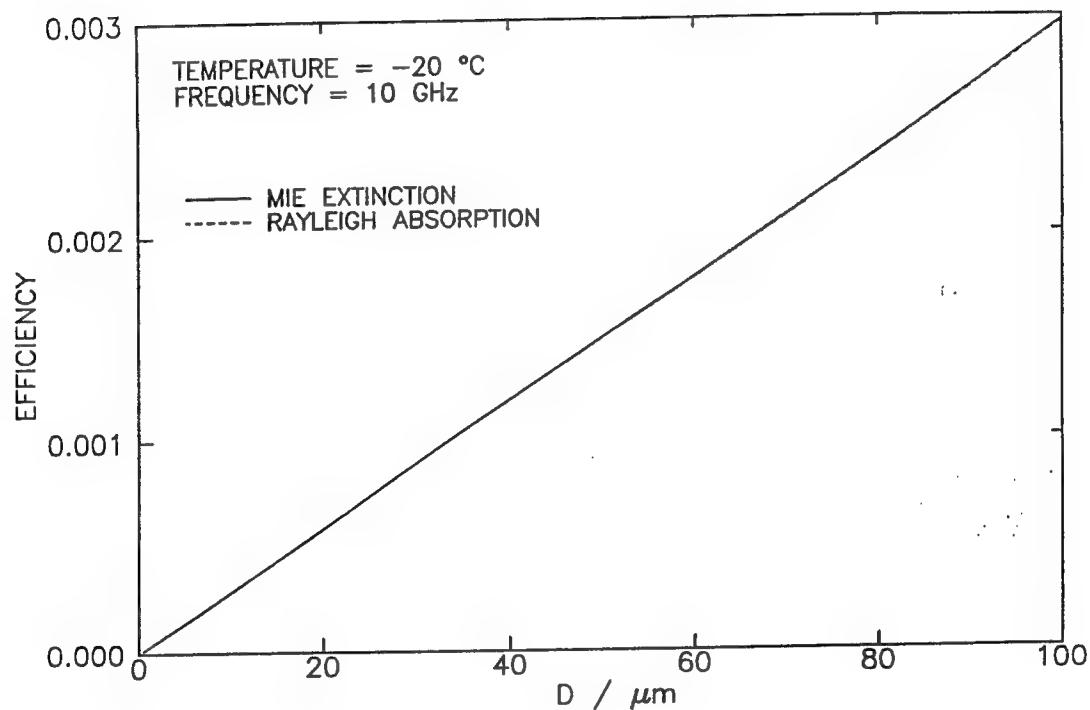
Figure 4a. Raleigh absorption efficiency and Mie extinction efficiency versus water drop diameter for fog with D = 0.5 − 100 μm, f = 10 GHz, and T = -20 °C.
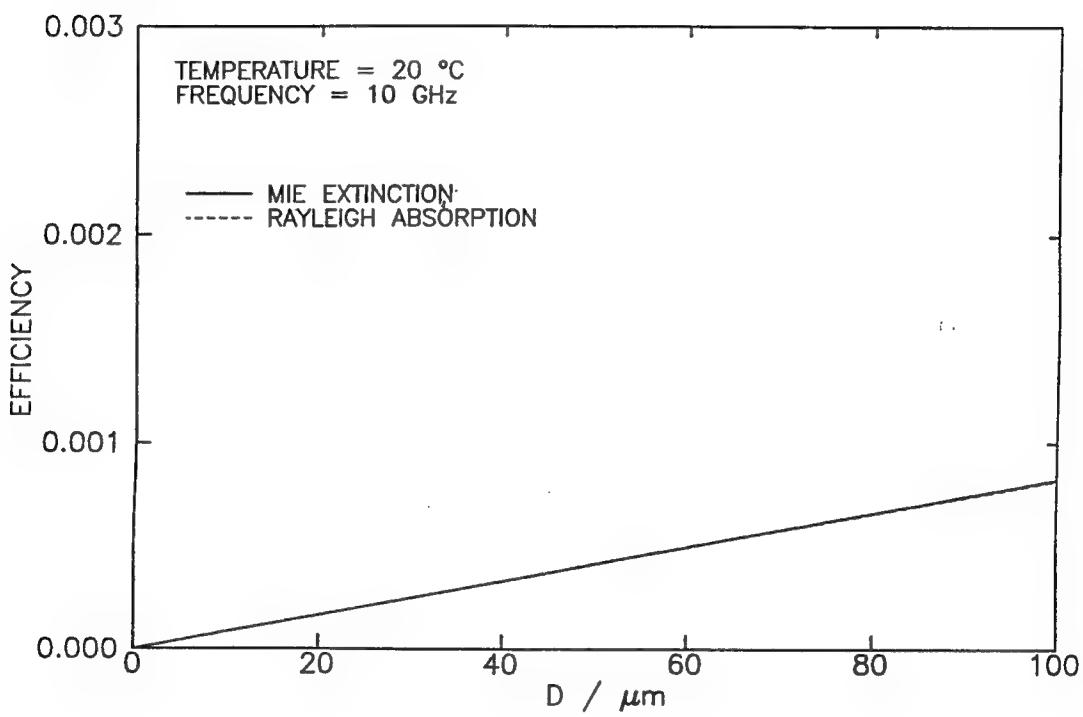
Figure 4b. Rayleigh absorption efficiency and Mie extinction efficiency versus water drop diameter for fog with D = 0.5 — 100 μm, f = 10 GHz, and T = 20 °C.
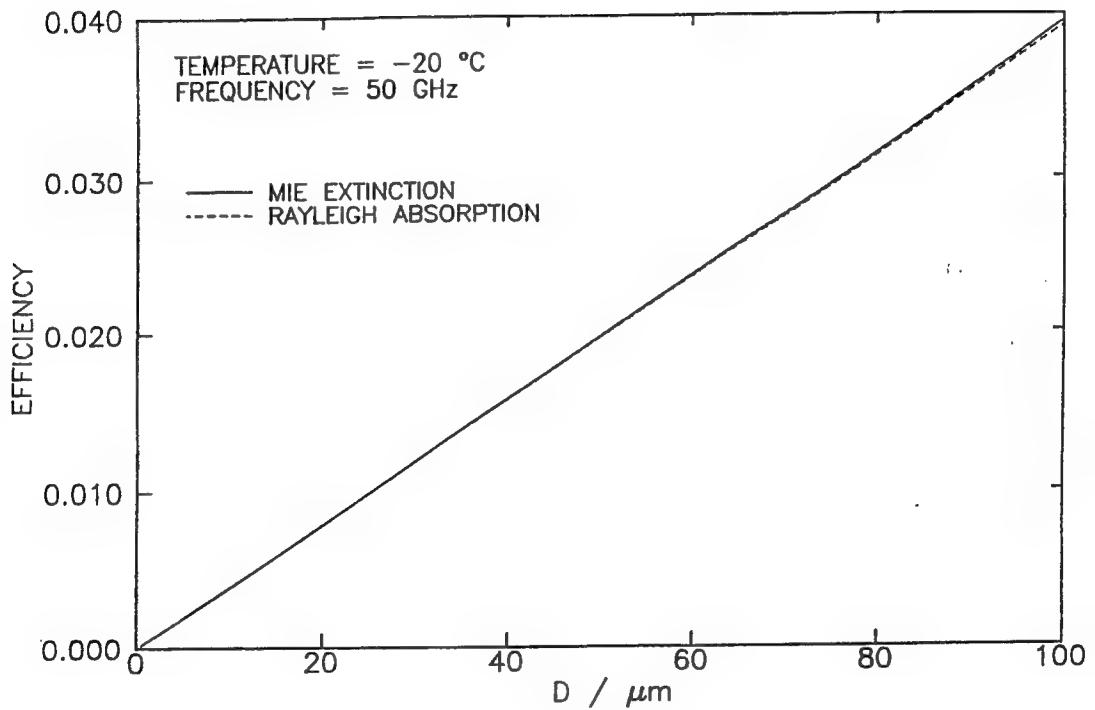
Figure 5a. Raleigh absorption efficiency and Mie extinction efficiency versus water drop diameter for fog with D = 0.5 — 100 μm, f = 50 GHz, and T = -20 °C.
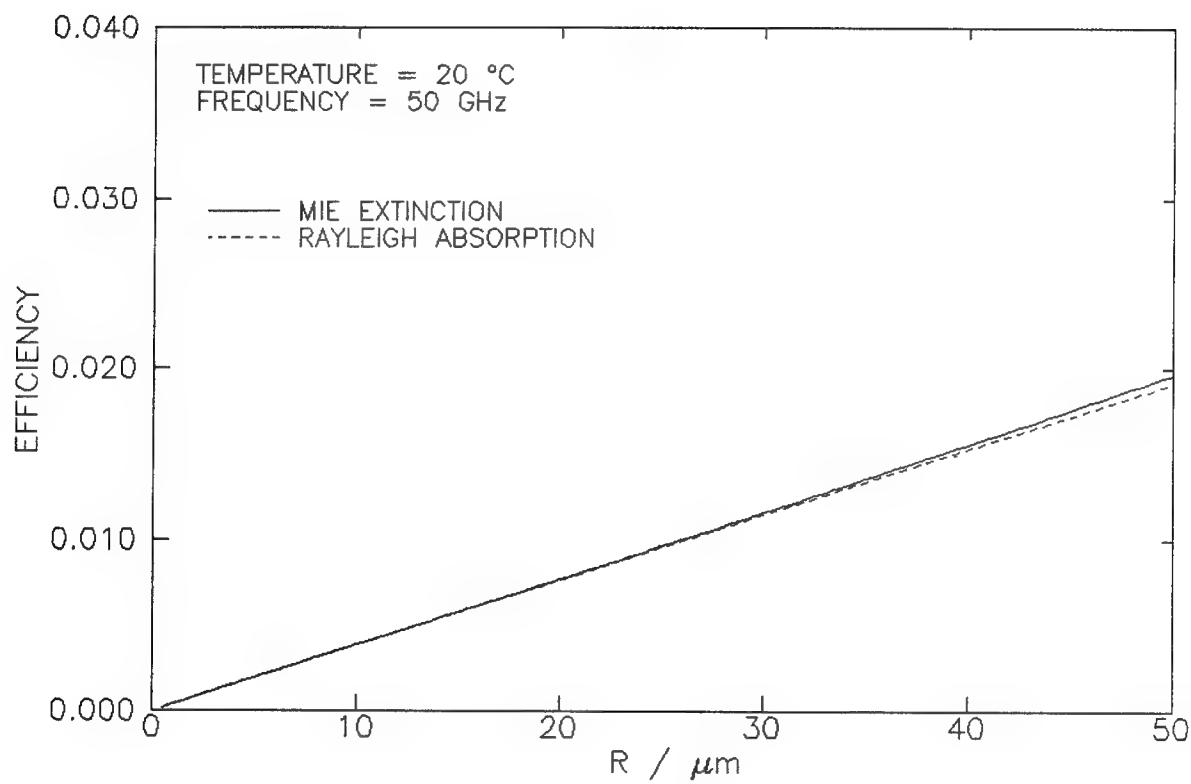
Figure 5b. Rayleigh absorption efficiency and Mie extinction efficiency versus water drop radius for fog with R = 0.5 — 50 μm, f = 50 GHz, and T = 20 °C.
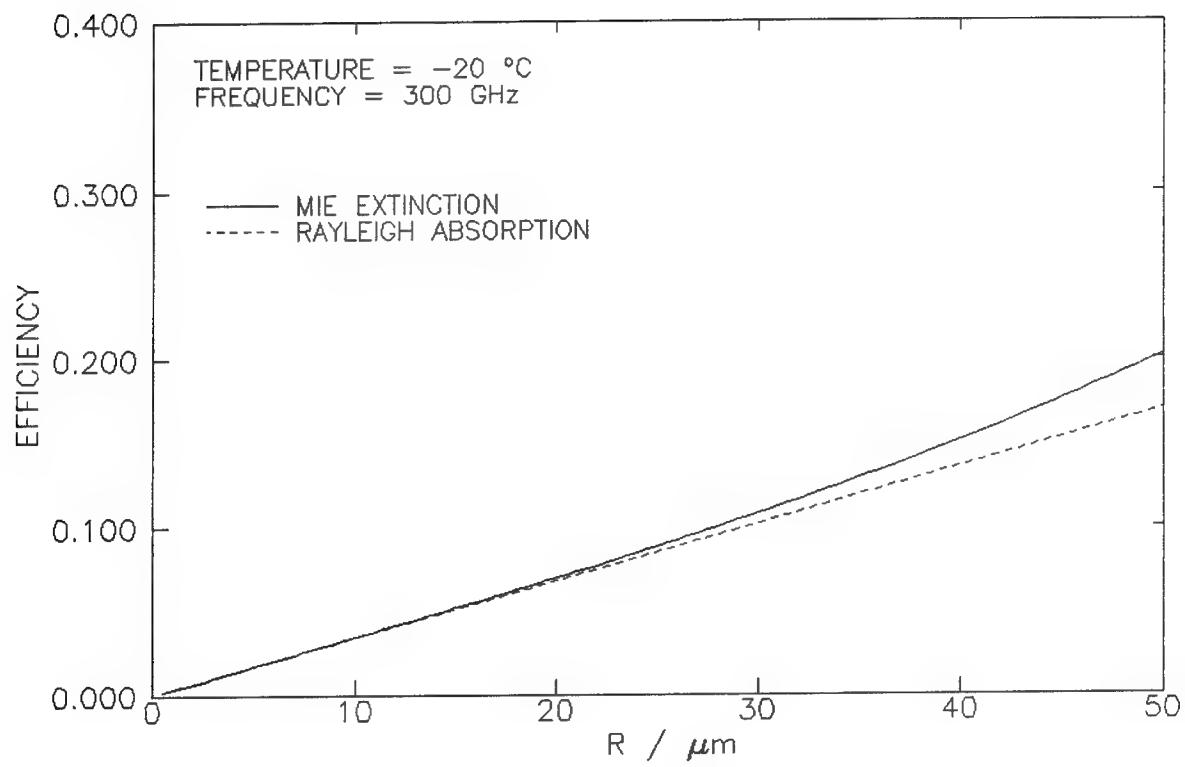
Figure 6a. Rayleigh absorption efficiency and Mie extinction efficiency versus water drop radius for fog with R = 0.5 — 50 μm, f = 300 GHz, and T = -20 °C.

24
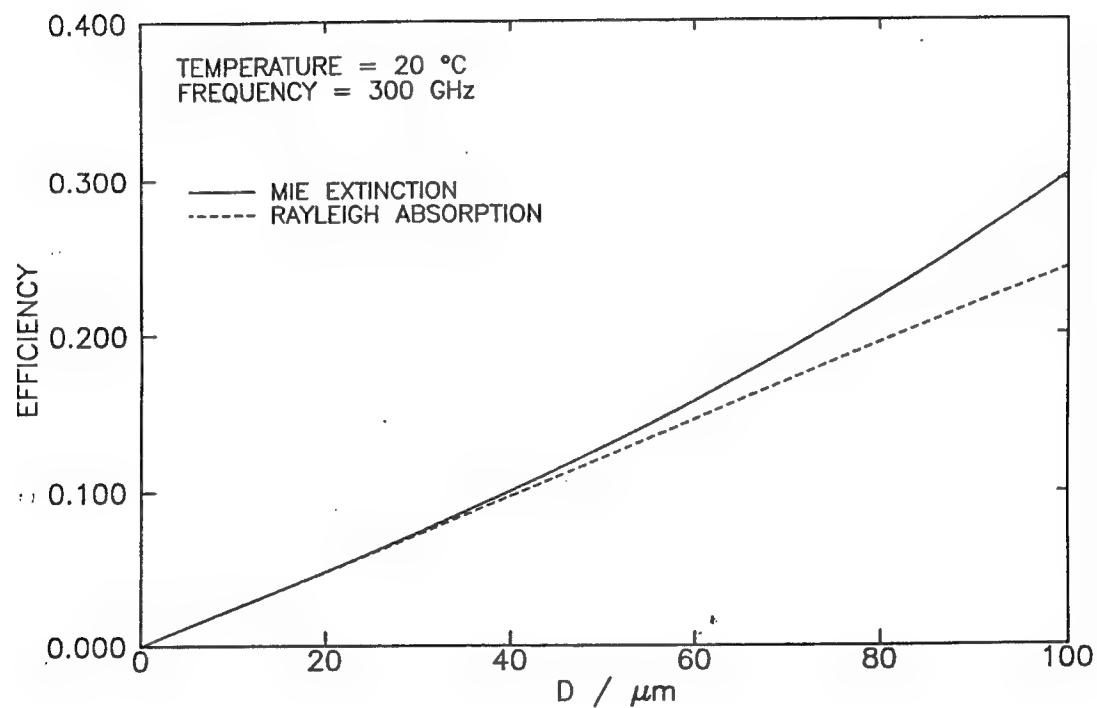
Figure 6b. Rayleigh absorption efficiency and Mie extinction efficiency versus water drop diameter for fog with $D = 0.5 - 100$ μm, $f = 300$ GHz, and $T = 20$ °C.
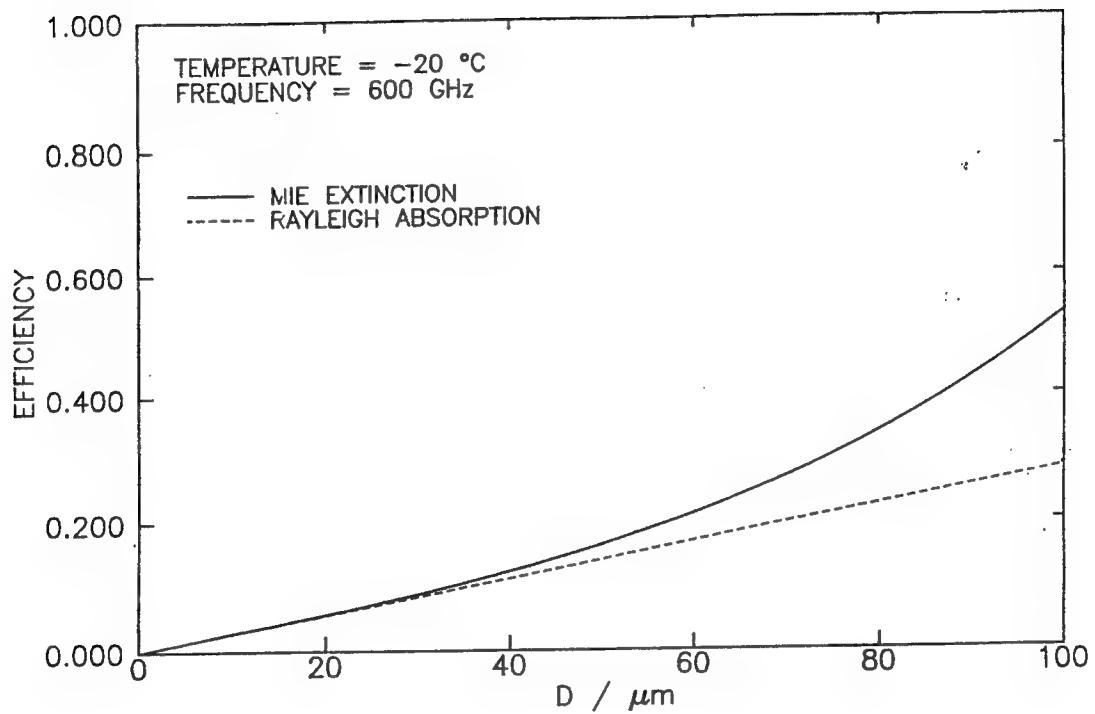
Figure 7a. Rayleigh absorption efficiency and Mie extinction efficiency versus water drop diameter for fog with D = 0.5 — 100 μm, f = 600 GHz, and T = -20 °C.
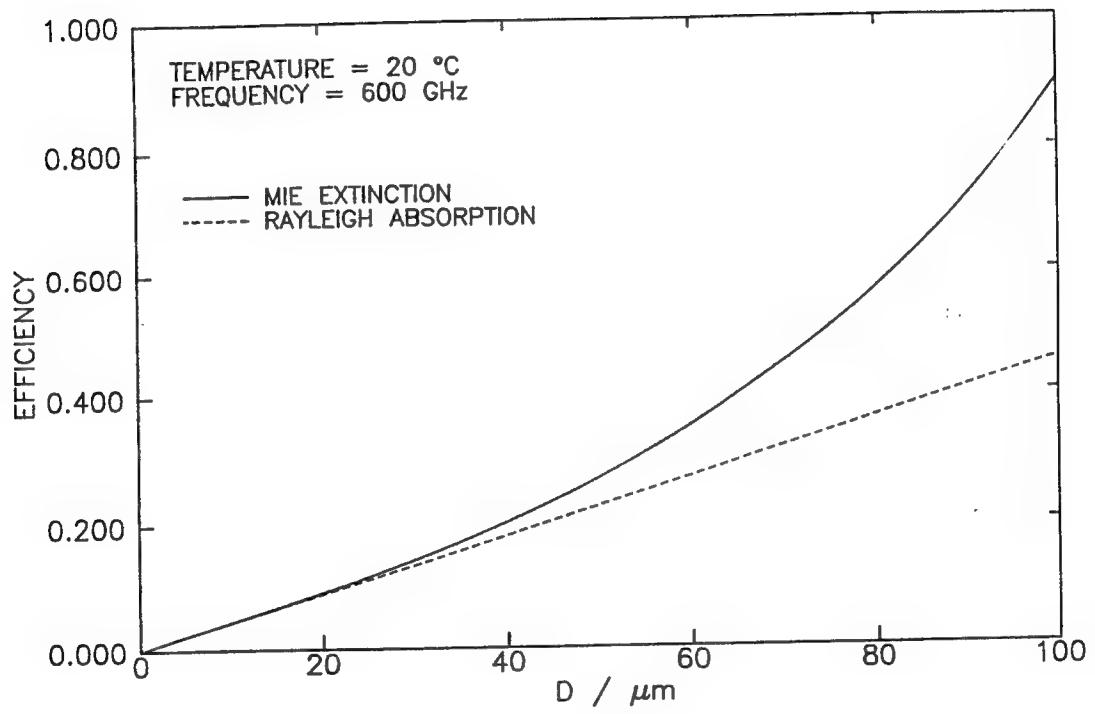
Figure 7b. Rayleigh absorption efficiency and Mie extinction efficiency versus water drop diameter for fog with D = 0.5 — 100 μm, f = 600 GHz, and T = 20 °C.
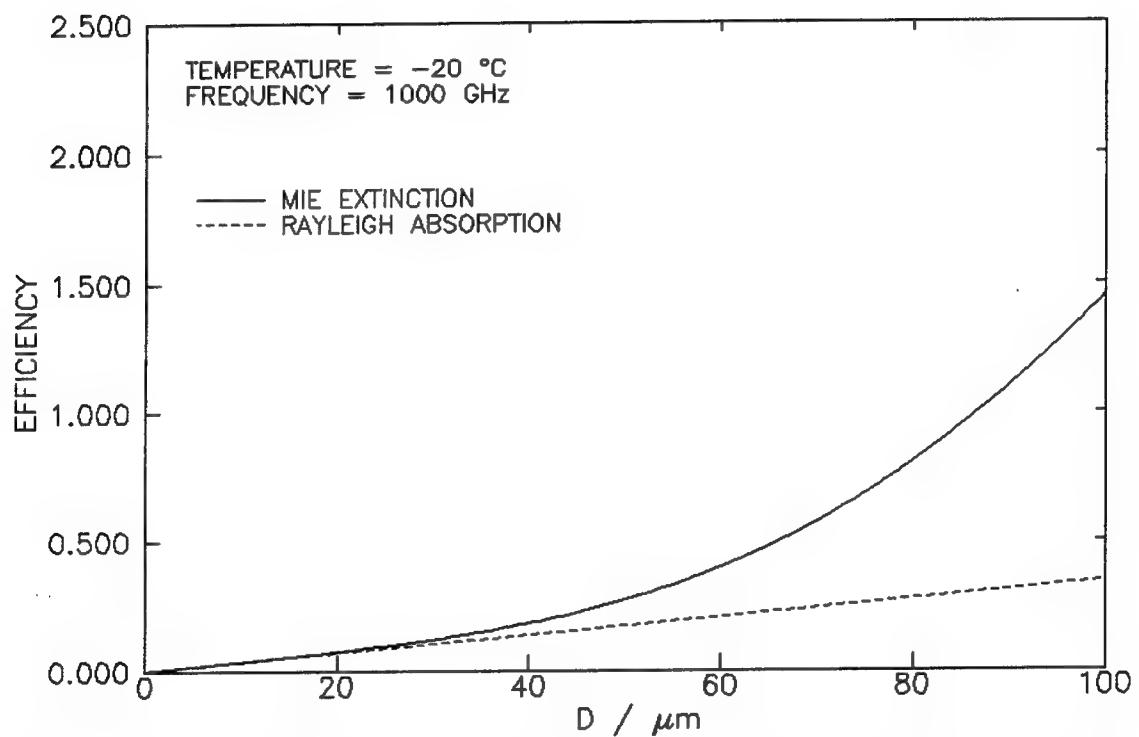
Figure 8a. Rayleigh absorption efficiency and Mie extinction efficiency versus water drop diameter for fog with D = 0.5 — 100 μm, f = 1000 GHz, and T = -20 °C.
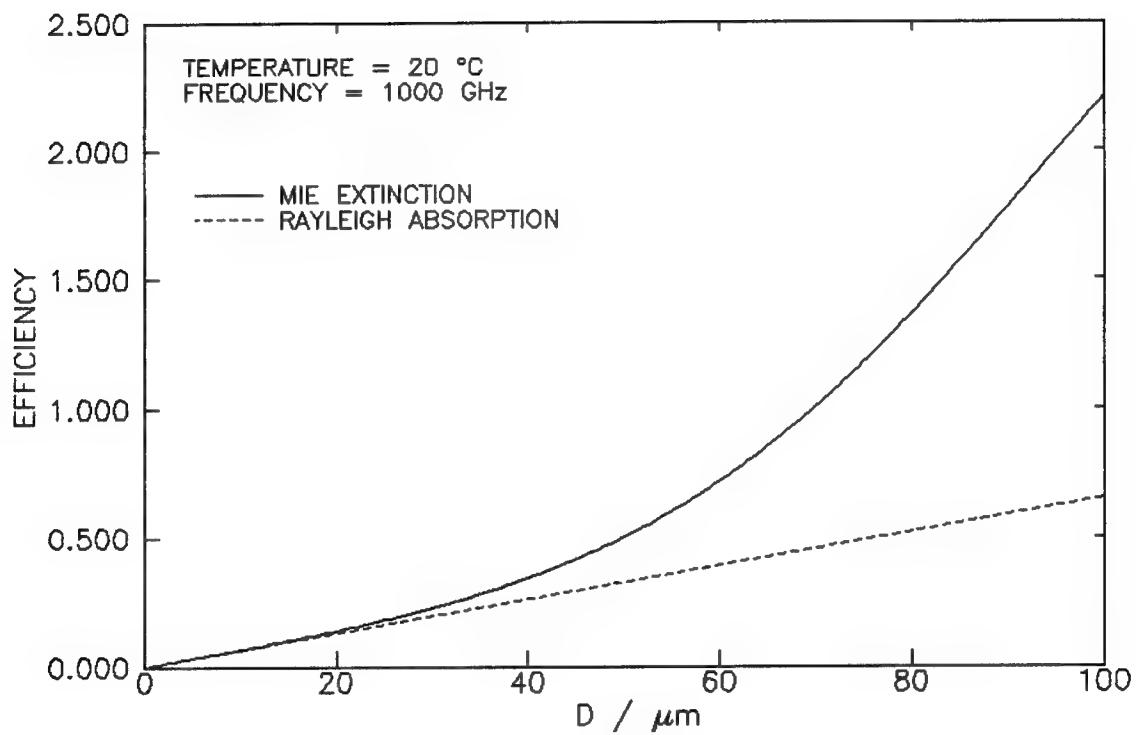
**Figure 8b.** Rayleigh absorption efficiency and Mie extinction efficiency versus water drop diameter for fog with D = 0.5 — 100 μm, f = 1000 GHz, and T = 20 °C.

7. Attenuation Caused by Rain With an MP Size Distribution

Section 6 demonstrated that for fog with maximum diameters of 100 μm, Rayleigh theory is essentially exact at microwave frequencies of 1 – 10 GHz. This was done by comparing the Rayleigh absorption efficiency with the Mie extinction efficiency over a size range of spherical water droplets up to 100 μm in diameter. This section will discuss the sphericity of rain drops; in addition, it will be determined whether Rayleigh approximation can be used for rain drops in the microwave frequency range of 1 – 10 GHz.

Evidence suggests that rain drops can be significantly nonspherical. Therefore, it is common to introduce an equivalent diameter, D_0, defined as the diameter of a sphere with the same volume as the nonspherical drop. This approach was taken by Pruppacher and Klett who gave a succinct discussion of rain drop shapes:

> When falling at terminal velocity, drops are nearly perfect spheres if $D_0 < 280$ μm. Larger drops are slightly deformed and resemble oblate spheroids if 280 μm $< D_0 < 1000$ μm. For $D_0 > 1000$ μm, the deformation becomes large and the drops resemble oblate spheroids with flat bases. Drops larger than about 10 mm in diameter are hydrodynamically unstable and break up, even in a laminar air stream. [4]

Pruppacher and Klett's discussion shows that a nearly exact description of rain drops is likely to be extremely difficult, requiring full time research by specialists who study the production and mechanics of nonspherical rain drops. Appropriate electromagnetic scattering algorithms which can compute Q_{ext} for nonspherical drops are also required. The results are orientation dependent and require averaging over angles which describe the orientation. The situation is even worse if the drop orientations are not isotropic but have preferred orientations. With all these considerations and difficulties in mind, it becomes obvious why the assumption of a simple size distribution of equivalent spheres is usually made. Therefore, the given analysis of attenuation by rain will assume spherical drops.

The question is whether the Rayleigh approximation can be used for rain drops by comparing the Rayleigh absorption efficiency with the Mie

extinction efficiency over a size range of spherical rain drops up to 2.5 mm in the microwave frequency range of 1 – 10 GHz. This is done in figures 14 through 18 for frequencies of 1, 3, 5, and 10 GHz. These figures show that if f = 1 GHz, the Rayleigh approximation is within 20 percent; if f = 3 GHz, the Rayleigh result is still within an order of magnitude. This is not true as frequencies increase past 5 GHz. Failure to achieve order of magnitude agreement over the range of interest resulted in the investigation of the numerical integration of equation (10):

$$\alpha_{ext} = \frac{\pi}{4} \int_0^\infty Q_{ext} D^2 N \ dD. \qquad (10)$$

D represents an equivalent sphere diameter if the drops are nonspherical. If a size distribution of the rain drops is known or assumed, Q_{ext} can be calculated using Mie theory and equation (10) can be numerically integrated.

Oguchi [5] discusses of the issues related to nonspherical drops. Discussion is made of two commonly used size distributions of equivalent spheres: 1) Laws and Parsons and 2) MP. Oguchi performed the numerical integration of these two distributions and thereby produced curves of specific attenuation (i. e., dB/km) as a function of frequency with f = 1 – 1000 GHz at T = 20 ˚C. Curves were produced for rain rates R = 2.5, 12.5, 50, and 150 mm/h. According to the National Weather Service Weather Radar Code, [6] rain rates are classified as light (0 – 3.8 mm/h), moderate (3.8 – 20 mm/h), strong (20 – 40 mm/h), very strong (40 – 76 mm/h), intense (76 – 152 mm/h), and extreme (greater than 152 mm/h).
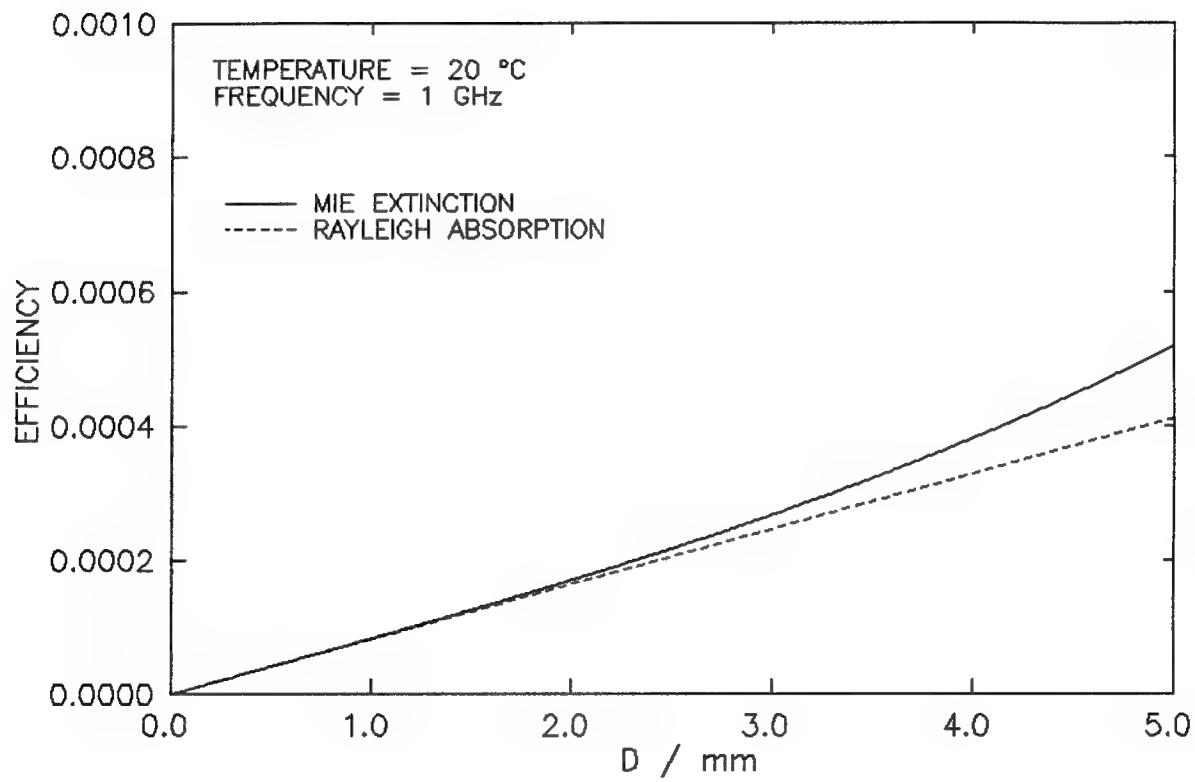
**Figure 9.** Rayleigh absorption efficiency and Mie extinction efficiency versus water drop diameter for rain with D = 0.05 — 5.0 mm, f = 1 GHz, and T = 20 °C.
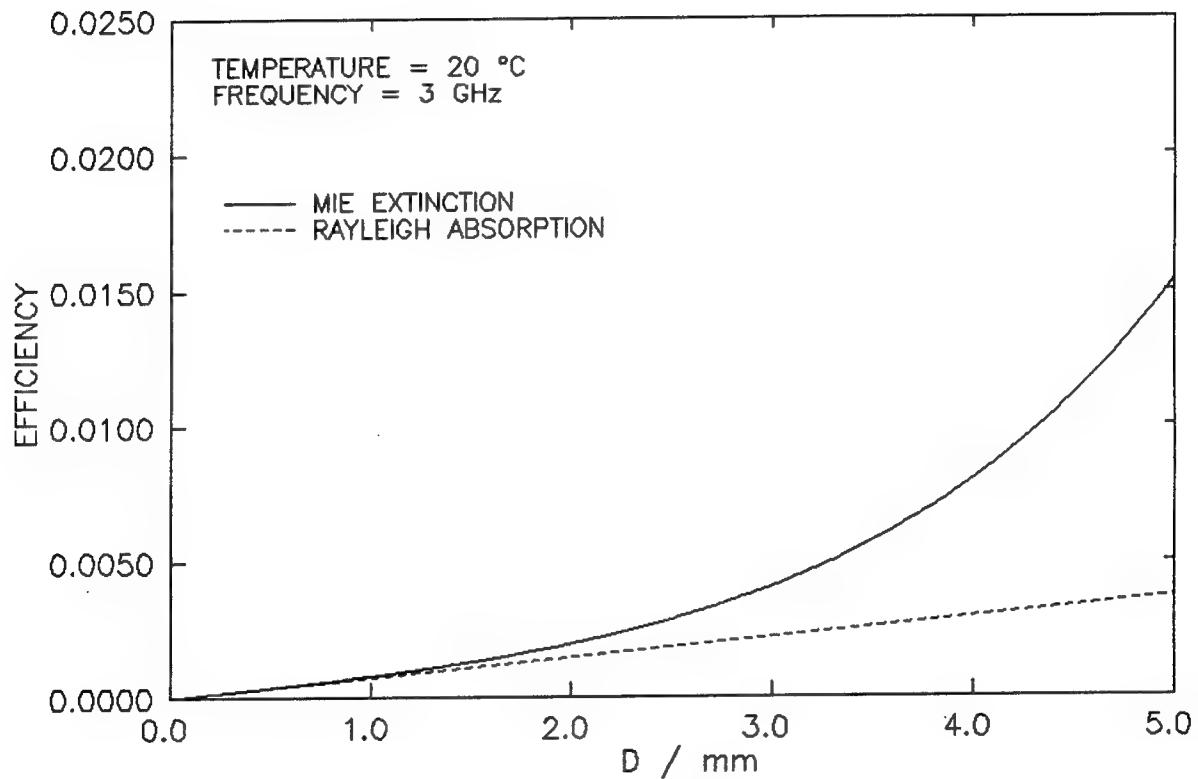
**Figure 10.** Rayleigh absorption efficiency and Mie extinction efficiency versus water drop diameter for rain with D = 0.05 — 5.0 mm, f = 3 GHz, and T = 20 °C.
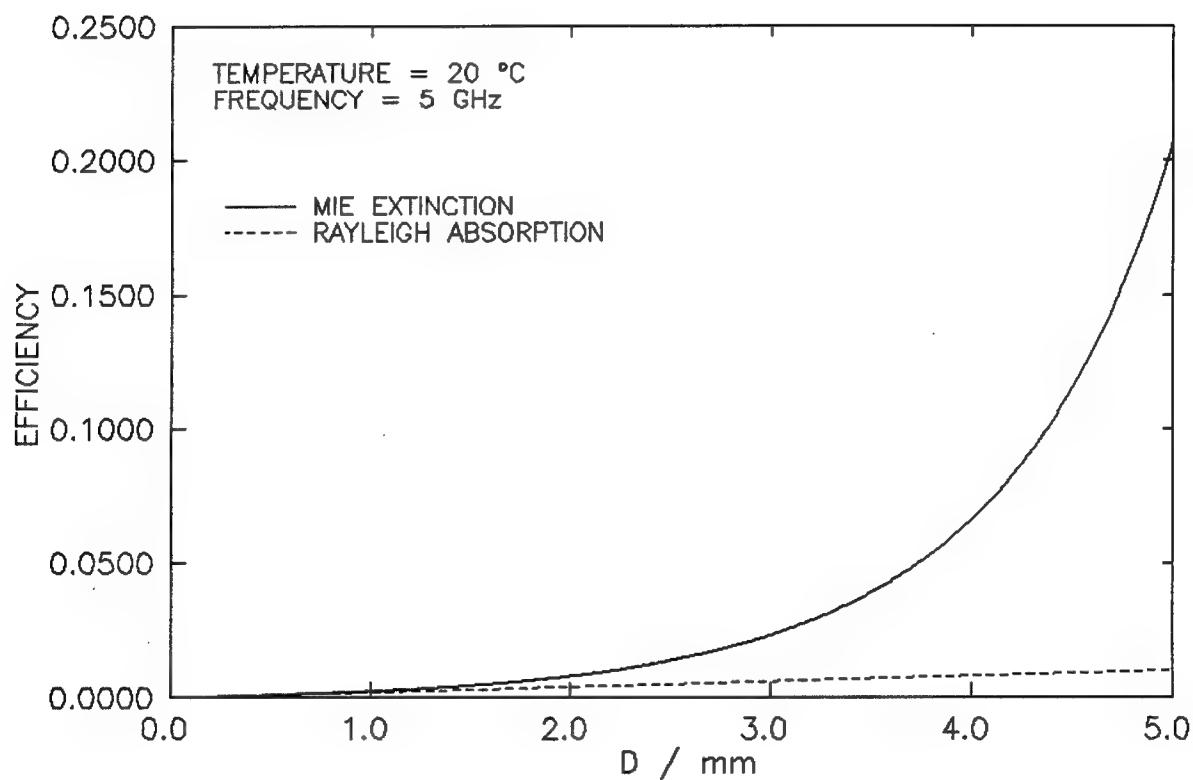
Figure 11. Rayleigh absorption efficiency and Mie extinction efficiency versus water drop diameter for rain with D = 0.25 — 5.0 mm, f = 5 GHz, and T = 20 °C.
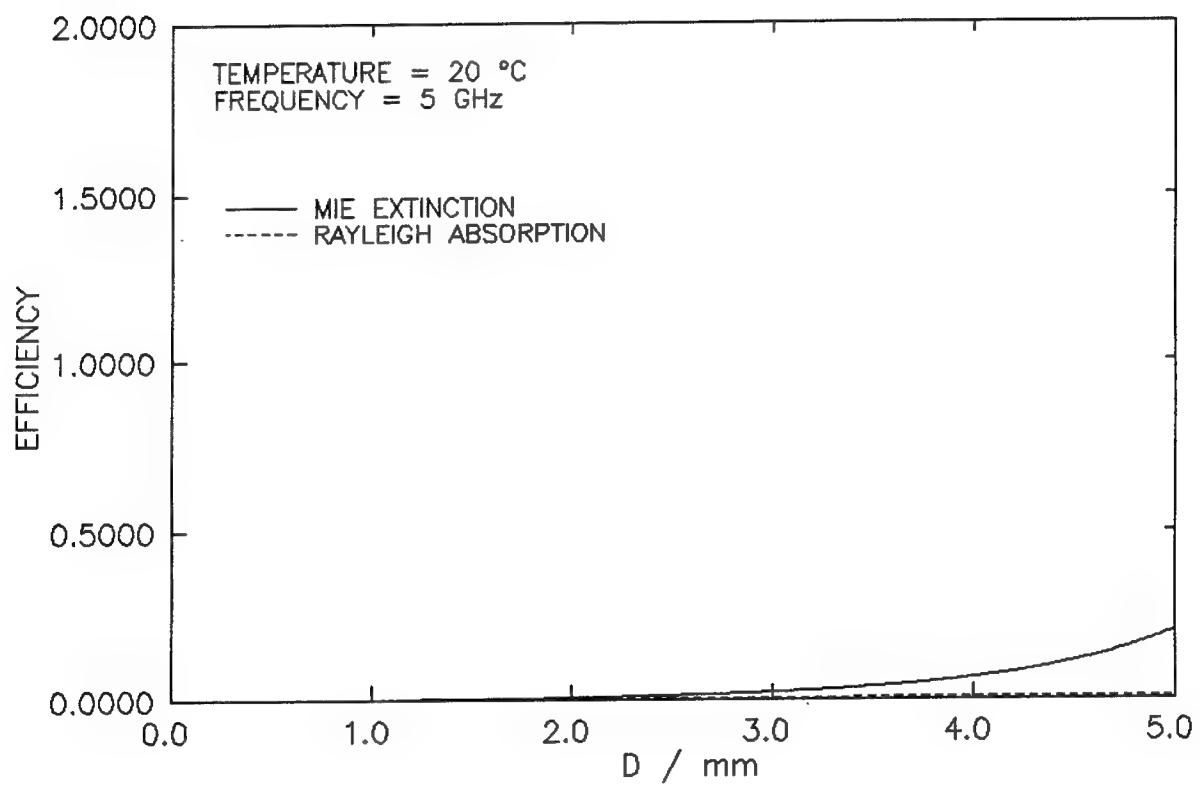
Figure 12. Rayleigh absorption efficiency and Mie extinction efficiency versus water drop diameter for rain with D = 0.05 — 5.0 mm, f = 5 GHz, and T = 20 °C (scaled differently to facilitate comparison with figure 13).
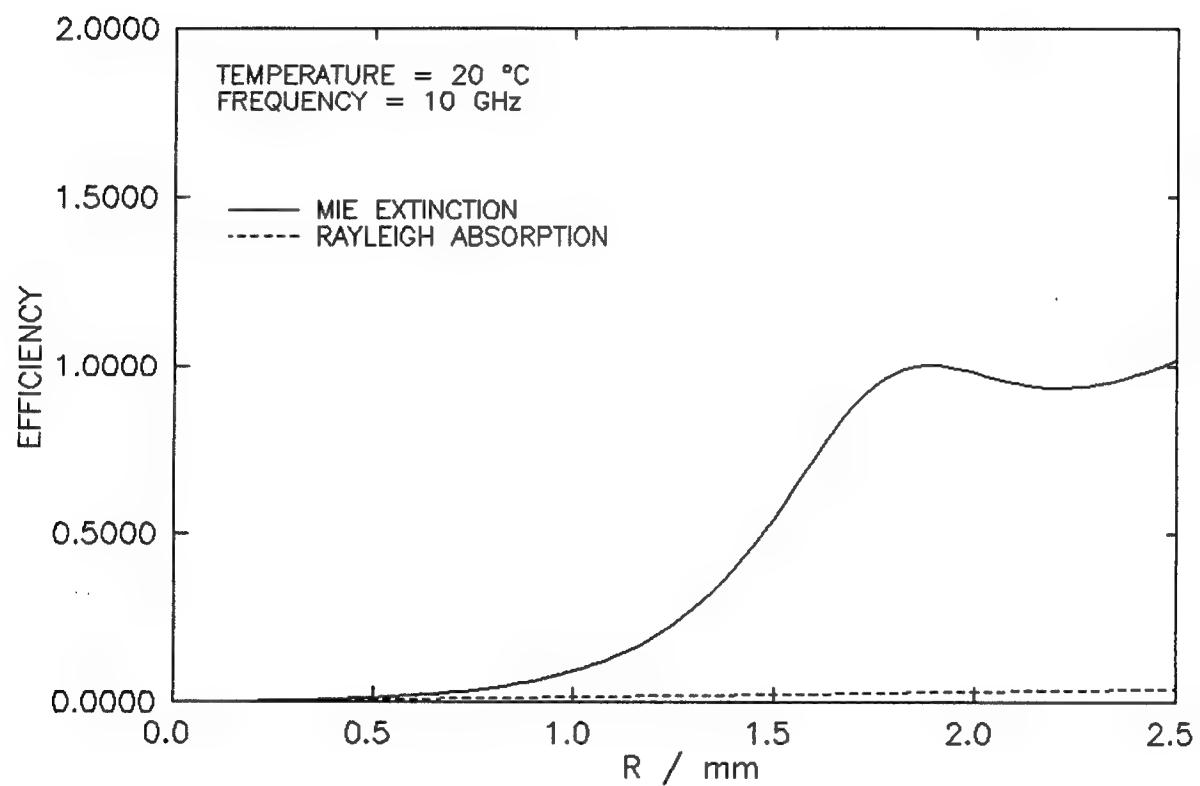
**Figure 13.** Rayleigh absorption efficiency and Mie extinction efficiency versus water drop diameter for rain with R = 0.025 — 2.5 mm, f = 10 GHz and T = 20 °C.

At Army Research Laboratory (ARL), a code employing numerical integration of equation (10) has been developed; Oguchi's specific attenuation curves [5] for the MP size distribution are reproduced in figure 19. Comparison of Oguchi's original and the reproduction shows close agreement.

Brown [1] makes the comment that full Mie scattering calculations are too cumbersome for inclusion in the EOSAEL. As an alternative procedure, Brown uses the following power law relationship developed by ORH: [7]

$$\alpha = aR^b, \tag{29}$$

where a and b were determined for various size distributions, including the MP distribution used in the numerical calculations of this report. The ORH coefficients (a and b) are listed in tabular form as a function of frequency for 41 frequencies between 1 and 1000 GHz at temperatures of -10, 0, and 20 °C. The ORH MP coefficients for T = 20 °C were used to compute ORH attenuation coefficients for comparison with the integrated Mie theory results of figure 19. The results of this comparison are shown in figure 20. The ORH results shown at the 41 discrete frequencies of their table agree with the results given in figure 19 for rain rates less than or equal to 50 mm/h. More deviation is seen for the highest rain rate of 150 mm/h. Figure 21 shows the same comparison except that only frequencies less than 10 GHz are considered and the same trend is observed (i.e., better agreement is obtained for the lower rain rates). These computations are repeated in figures 22 through 24 for T = 0 °C with essentially the same result (i.e., better agreement at the lower rain rates). In EOSAEL 82 to 84, Brown [1] used the ORH MP coefficients [7] for a rain rate of 4 mm/h, which proved to be appropriate. The main problem with depending on the ORH approach is that the coefficients are only available for T = -10, 0, and 20 °C; however, the full Mie scattering calculations are not cumbersome and are easy to produce.
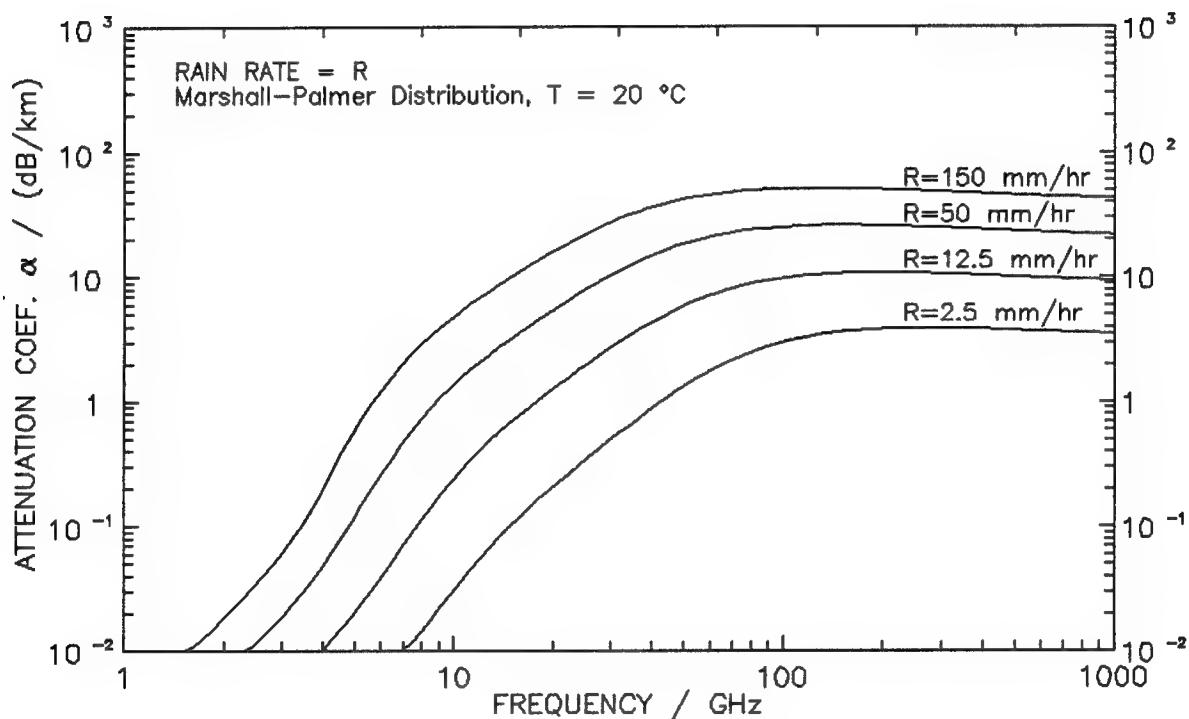
Figure 14a. Attenuation coefficient α of rain versus frequency for f = 1 — 1000 GHz; computed for rain rates R = 2.5 — 150 mm/h using numerical integration of the MP distribution with T = 20 °C.

39
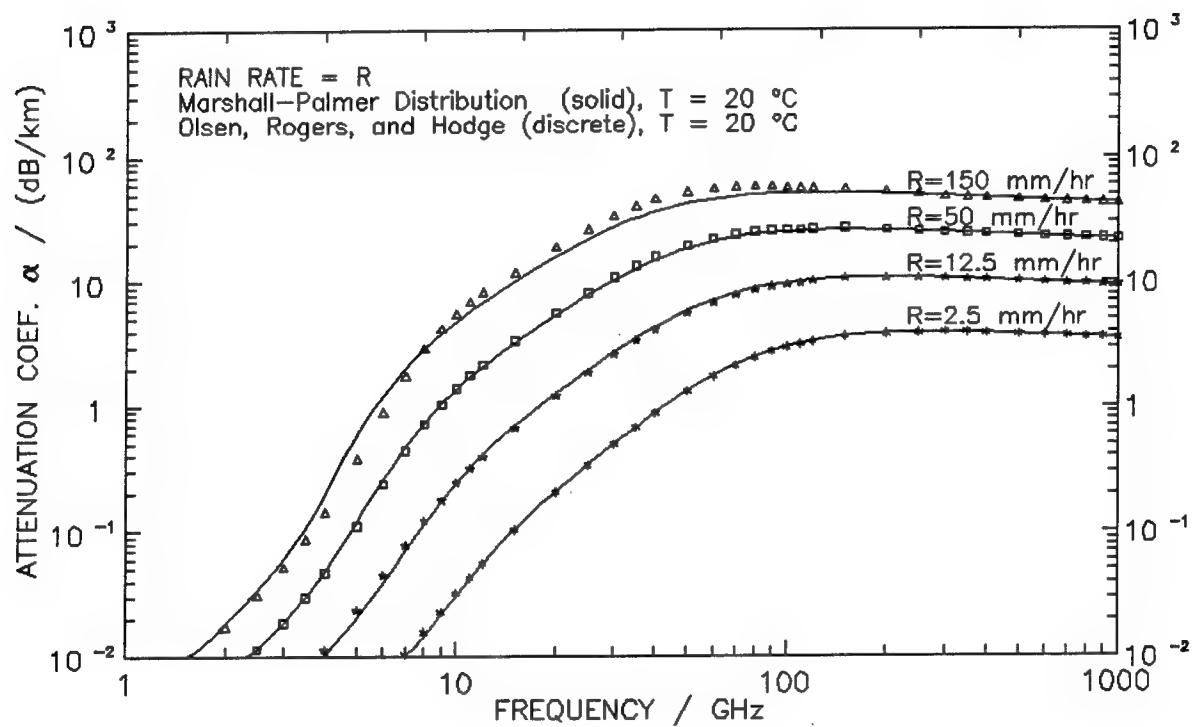
Figure 14b. Attenuation coefficient α of rain versus frequency for $f = 1 - 1000$ GHz; compares numerical integration of the MP distribution $(T = 20\ °C)$ with discrete points given by the ORH equation $(T = 20\ °C)$.

40
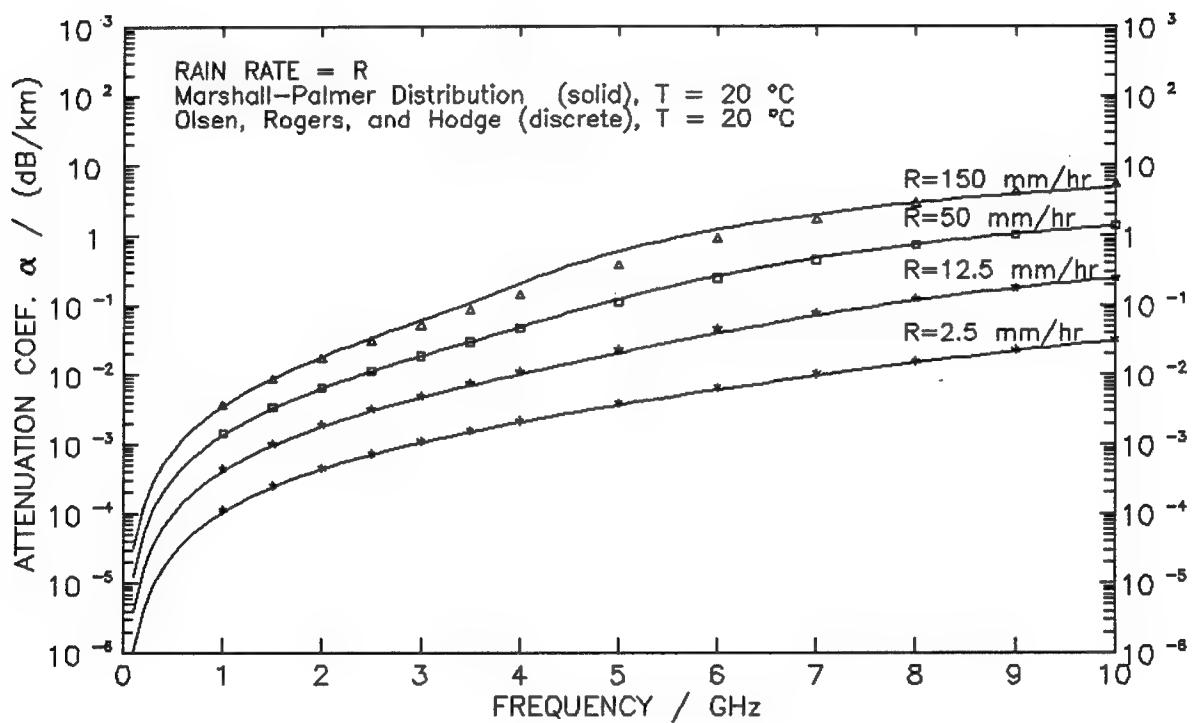
Figure 14c. Attenuation coefficient α of rain versus frequency for $f = 0.1 - 10$ GHz; compares numerical integration of the MP distribution $(T = 20\ °C)$ with discrete points given by the ORH equation $(T = 20\ °C)$.

41
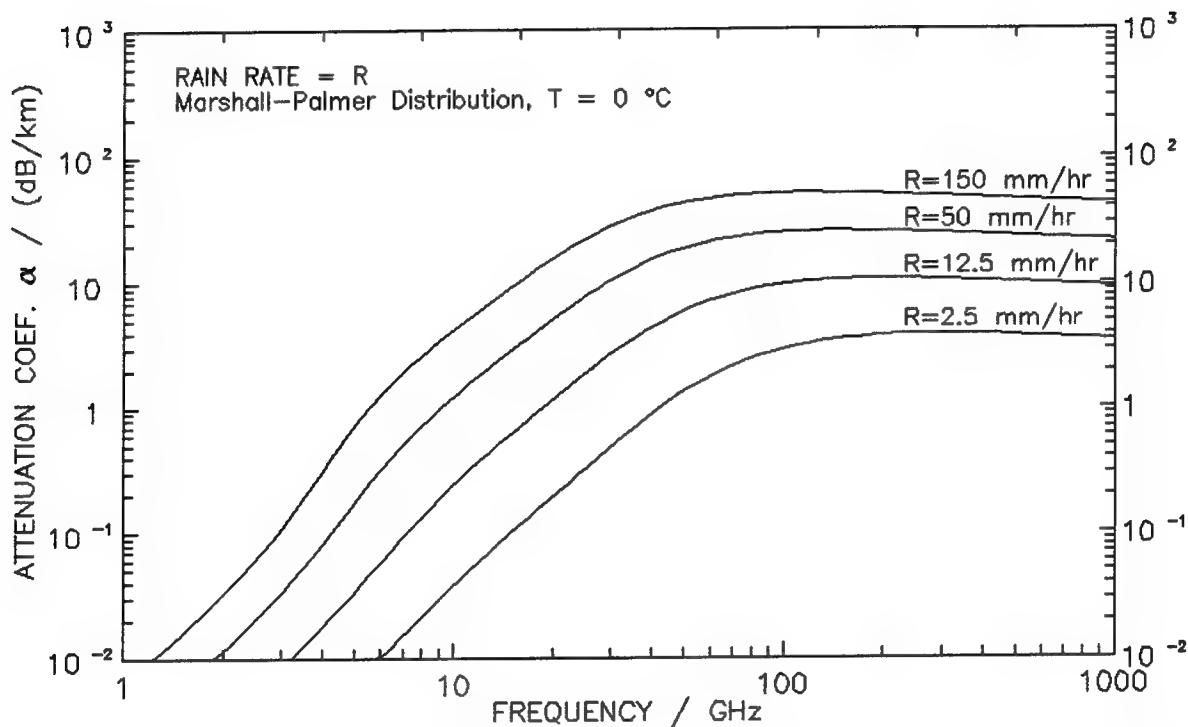
Figure 15a. Attenuation coefficient α of rain versus frequency for $f = 1 - 1000$ GHz; computed for rain rates $R = 2.5 - 150$ mm/h using numerical integration of the MP distribution with $T = 0$ °C.
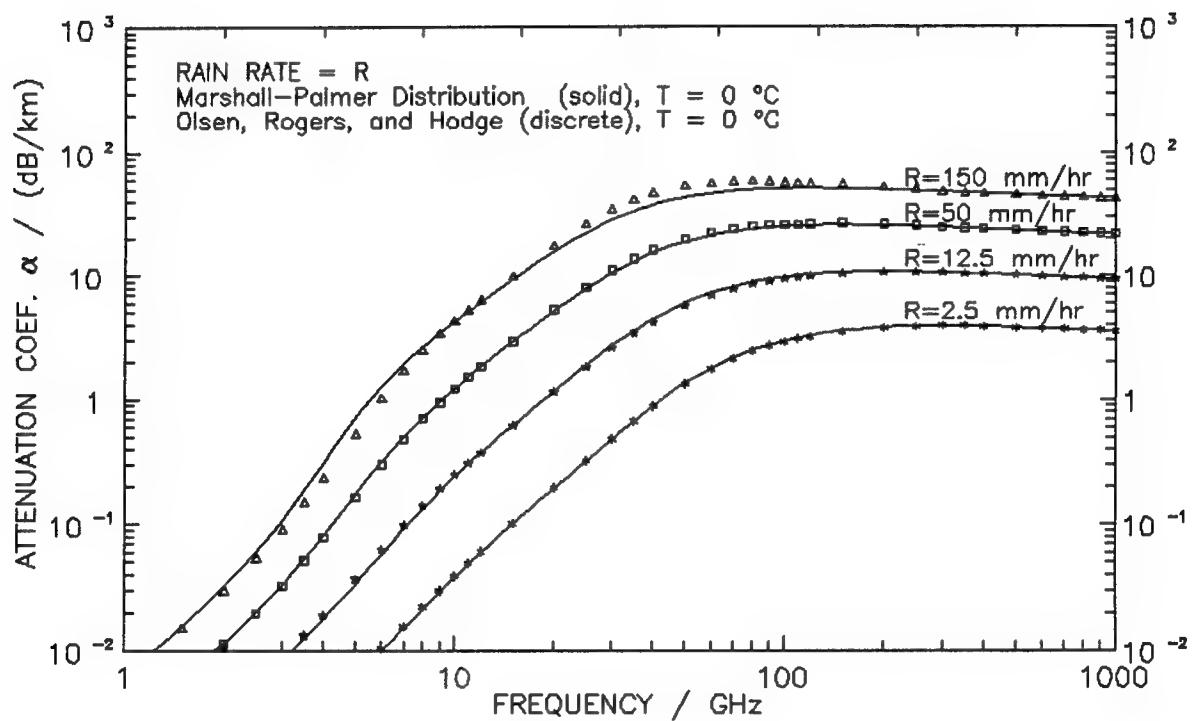
Figure 15b. Attenuation coefficient α of rain versus frequency for $f = 1 - 1000$ GHz; compares numerical integration of the MP distribution $(T = 0\ °C)$ with discrete points given by the ORH equation $(T = 0\ °C)$.
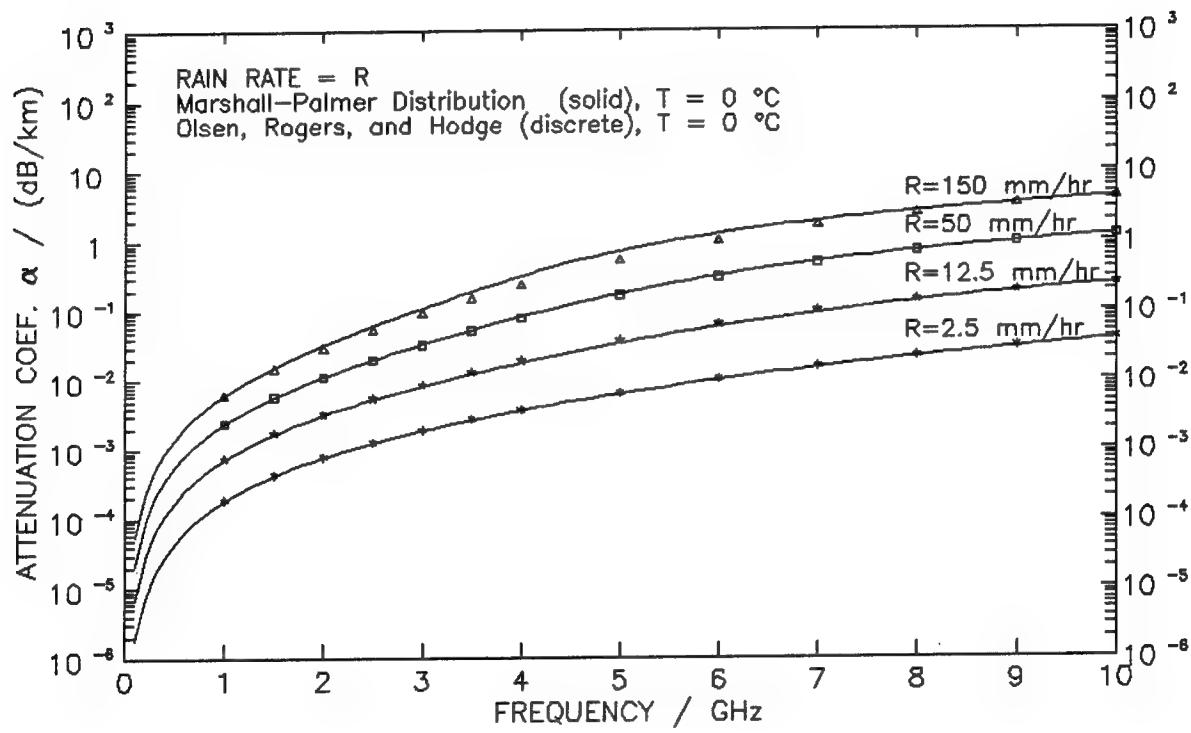
Figure 15c. Attenuation coefficient α of rain versus frequency for $f = 0.1 - 10$ GHz; compares numerical integration of the MP distribution $(T = 0\ °C)$ with discrete points given by the ORH equation $(T = 0\ °C)$.

44

Deviation with increasing temperature is demonstrated by figures 25 and 26; these show integrated Mie theory attenuation coefficients for $T = 40$ and $60\ ^{\circ}$C. In these figures, the ORH attenuation coefficients at 20 $^{\circ}$C are shown for comparison. For the lower rain rates, figure 25 shows the Mie attenuation at 40 $^{\circ}$C becomes lower than that given by ORH at 20 $^{\circ}$C. However, agreement for the higher rain rates is better.

Use of ORH coefficients is a good method for avoiding numerical integration. However, once a code is obtained, it is quick and easy to find attenuation coefficients by performing numerical integration of the Mie theory over the size distribution of interest.

For a sample calculation of attenuation by rain, $f = 10$ GHz and $T = 20\ ^{\circ}$C, figure 21 gives the result that $\alpha = 5$ dB/km when $R = 150$ mm/h. At a range of 1 km, $\alpha z = 5$ dB and equation (5) gives $I(z)/I(z=0) = 10^{-0.5} = 0.316$. At ranges of 1 km, an intense rain is seen to cause attenuation of about 68 percent, still less than an order of magnitude.
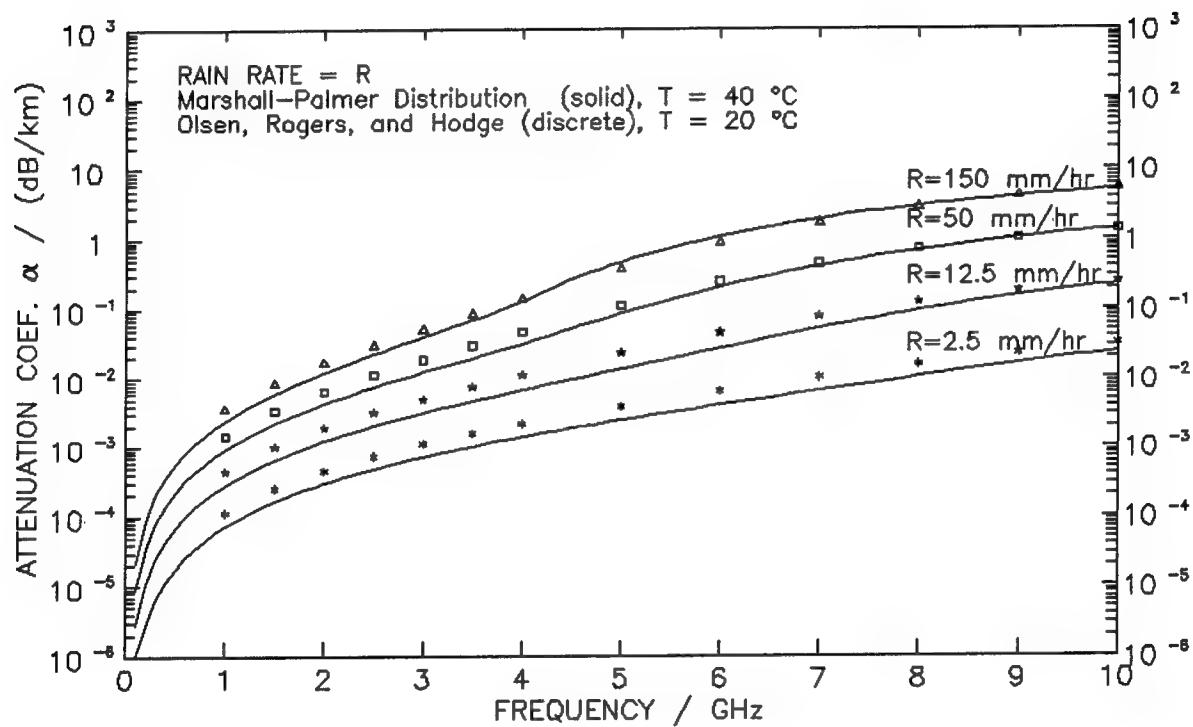
Figure 16. Attenuation coefficient α of rain versus frequency for f = 0.1 — 10 GHz; compares numerical integration of the MP distribution (T = 40 °C) with discrete points given by the ORH equation (T = 20 °C).

46
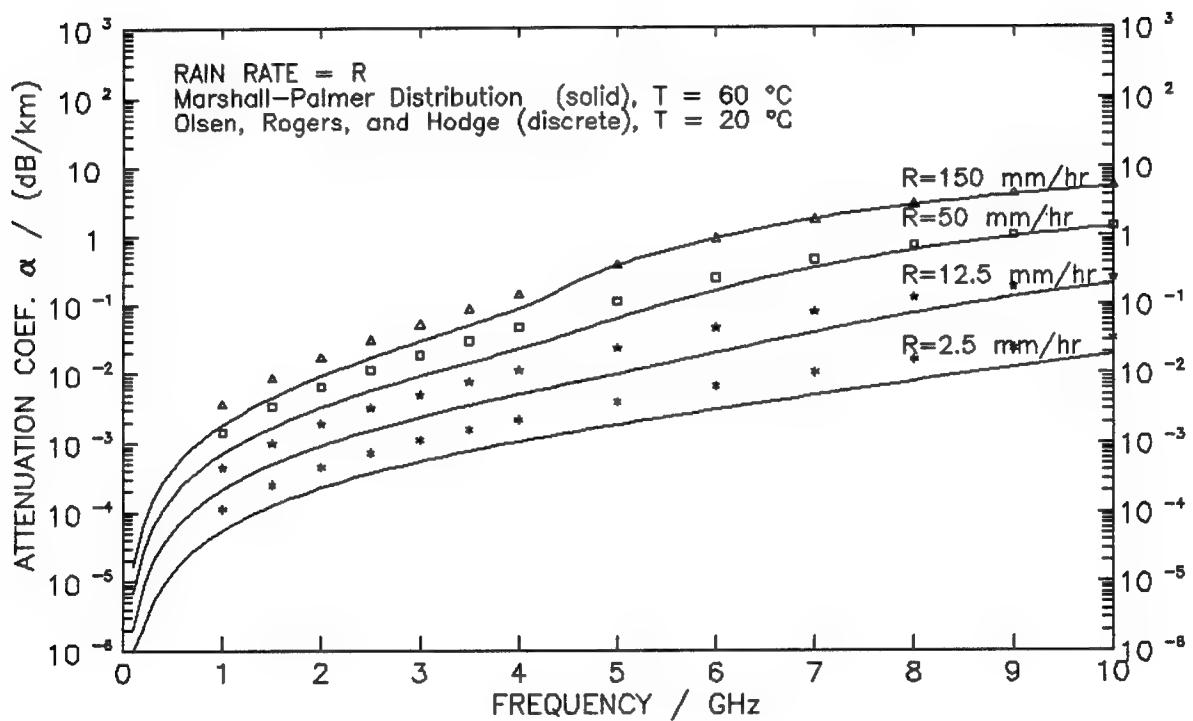
Figure 17. Attenuation coefficient α of rain versus frequency for f = 0.1 — 10 GHz; compares numerical integration of the MP distribution (T = 60 °C) with discrete points given by the ORH equation (T = 20 °C).

8. Summary

In this report, the equations which describe the attenuation of long-wavelength electromagnetic radiation by rain and fog were briefly reviewed and explained under the assumption that the aerosol droplets were spherical and that the irradiance of the beam was in the linear regime.

Calculations of water fog attenuation coefficients were made using the Rayleigh (i.e., small particle) approximation; an error analysis of this approximation was made by comparing Rayleigh approximation calculations of absorption efficiency with exact Mie theory calculations of extinction efficiency. Rayleigh approximation is appropriate for fog with drop diameters up to 100 μm for frequencies less than 50 GHz. A comparison of Rayleigh absorption efficiencies with Mie extinction efficiencies for rain with water drops up to 5.0 mm was used to show that, for frequencies above 1 GHz, the use of the Rayleigh approximation for rain is not appropriate. Numerical integration of the Mie extinction efficiency was used to compute the attenuation coefficient for rain with an MP drop size distribution for various rain rates and temperatures. These results were compared with those given by a power law relationship with coefficients given by ORH; this was used in the NMMW Module of the EOSAEL. The ORH relationship gives very good results at temperatures where their coefficients were determined (from -20 to 20 °C). As temperature increases above 20 °C, the exact Mie calculations deviate increasingly from the results of ORH. Above 20 °C, the use of the ORH equation is not recommended. The exact Mie computations may easily be performed for any temperature; since this can be done easily on a personal computer, this approach is recommended.

References

1. Brown, D. R., *Near Millimeter Wave Module NMMW*, TR-0221-6, U.S. Army Atmospheric Sciences Laboratory EOSAEL 87:6, White Sands Missile Range, NM, 1987.

2. Bohren, C. R. and D. R. Huffman, *Absorption and Scattering of Light by Small Particles*. John Wiley and Sons: New York, 1983.

3. Liebe, H. J., T. Manabe, and G. A. Hufford, *IEEE Transactions on Antennas and Propagation:* 37:1617, 1989.

4. Pruppacher, H. R. and J. R. Klett, *Microphysics of Clouds and Precipitation*, Kluwer: Boston, 1980.

5. Oguchi, T., *Proceedings of the IEEE:* 71:1029, 1983.

6. Falcone, Jr., V. J., L. W. Abreu, and E. P. Shettle, *Atmospheric Attenuation of Millimeter and Submillimeter Waves: Models and Computer Code*, AFGL-TR-79-0253, Environmental Research Papers, No. 679, Air Force Geophysics Laboratory: Hanscom AFB, MA, 1979.

7. Olsen, R. L., D. V. Rogers, and D. B. Hodge, *IEEE Transactions on Antennas and Propagation*: AP-26:318, 1978.

Acronyms and Abbreviations

ARL	Army Research Laboratory
B	bel
C^3I	communications, command, control, and intelligence
dB	decibels
EMP	electromagnetic pulses
EOSAEL	Electro-Optical Systems Atmospheric Effects Library
MP	Marshall-Palmer
NMMW	Near Millimeter Wave
ORH	Olsen, Rogers, and Hodge

Appendix A

Calculation of the Complex Index of Refraction of Water for Frequencies $f = 0$ to 1000 GHz with the Double-Debye Formulation

The calculations of attenuation coefficient a done in this report as a function of frequency require that the complex index of refraction $\hat{N}$ be computed as a function of frequency. In the body of this report, $\hat{N}$ is represented for a harmonic wave with time-dependence exp(-iωt) as follows:

$$\hat{N} = Re(\hat{N}) + i\,Im(\hat{N}).$$ (A-1)

Liebe et al. [3] have given expressions for the complex permittivity of liquid water ε (relative to the air) at frequencies f = 0 to 1000 GHz using a double-Debye formulation. For time-dependence exp(-iωt), the relative complex permittivity is represented as follows:

$$\varepsilon = \varepsilon' + i\varepsilon.$$ (A-2)

The standard relation is as follows:

$$\hat{N} = (\mu\varepsilon)^{\frac{1}{2}},$$ (A-3)

where the magnetic permeability μ = 1 connects the real and imaginary components of $\hat{N}$ with those of ε and the result obtained is as follows:

$$Re(\hat{N}) = \left\{ \frac{1}{2}\left[\varepsilon' + \left[(\varepsilon')^2 + (\varepsilon'')^2 \right]^{\frac{1}{2}} \right] \right\}^{\frac{1}{2}}$$ (A-4)

$$Im(\hat{N}) = \frac{\varepsilon''}{2\,Re(\hat{N})}.$$ (A-5)

The absorption efficiency in the Rayleigh approximation is noted in the text of this report to be proportional to Im(Z) where the following is true:

$$Z = \frac{\hat{N}^2 - 1}{\hat{N}^2 + 2}.$$ (A-6)

For $\mu = 1$, this may be written in terms of the relative complex permittivity as follows:

$$Z = \frac{\varepsilon - 1}{\varepsilon + 2} \tag{A-7}$$

For calculations with a hand electronic calculator, it is useful to note the following:

$$Im(Z) = \frac{3\varepsilon''}{(\varepsilon' + 2)^2 + (\varepsilon'')^2}. \tag{A-8}$$

The double-Debye formulation of Liebe et al. [3] gives expressions for ε' and ε'' which can be used in equations A-4 and A-7:

$$\varepsilon' = (\varepsilon_0 - \varepsilon_1)\left[1 + \left(\frac{f}{f_p}\right)^2\right] + (\varepsilon_1 - \varepsilon_2)\left[1 + \left(\frac{f}{f_s}\right)^2\right] + \varepsilon_2 \tag{A-9}$$

$$\varepsilon'' = (\varepsilon_0 - \varepsilon_1)\left[1 + \left(\frac{f}{f_p}\right)^2\right]\left(\frac{f}{f_p}\right) + (\varepsilon_1 - \varepsilon_2)\left[1 + \left(\frac{f}{f_s}\right)^2\right]\left(\frac{f}{f_s}\right) \tag{A-10}$$

where

$$\varepsilon_0 = 77.66 + 103.3\,(\theta - 1)$$

$$\theta = \frac{300}{\dfrac{T}{^\circ C} + 273.15}$$

$$\varepsilon_1 = 5.48$$

$$\varepsilon_2 = 3.51$$

$$f_p = 20.09 - 142.4\,(\theta - 1) + 294\,(\theta - 1)^2\ \text{GHz}$$

$$f_s = 590 - 1500\,(\theta - 1)\ \text{GHz}.$$

Computations of $Re(\hat{N})$ and $Im(\hat{N})$ were done as a function of λ for T = 0, 20, and 40 °C. The results are shown in figures A-1 and A-2. Such calculations were earlier performed by Falcone et al. [6] in their figure 13. Comparison of these two sets of results shows agreement for $Re(\hat{N})$ and qualitative agreement for $Im(\hat{N})$, but quantitative differences exist for $Im(\hat{N})$. This is believed to be caused by Falcone et al.'s use of both log and linear scales in their figure 13. [6]
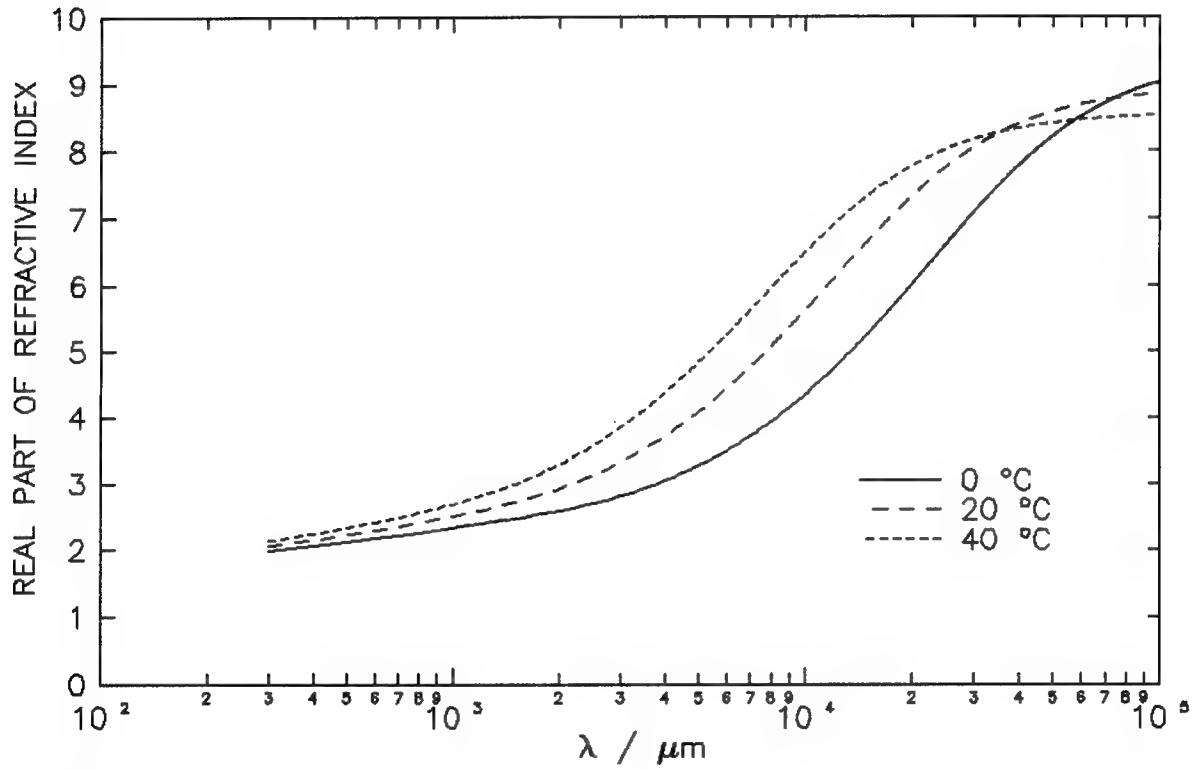
Figure A-1. **Real part of the complex index of refraction of water versus wavelength for** $\lambda = 10^2 - 10^5$ μm; **computed using the double-Debye expansion with** $T = 0 - 40$ °C.
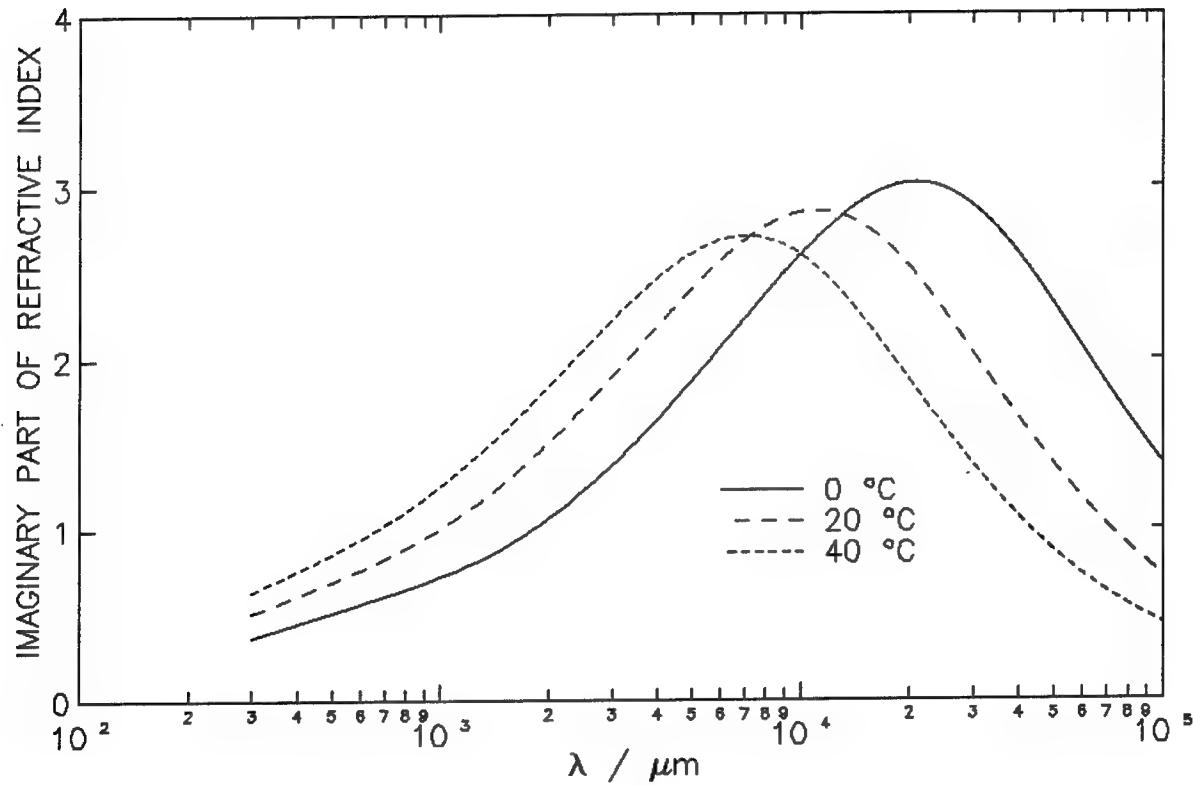
Figure A-2. Imaginary part of the complex index of refraction of water versus wavelength for $\lambda = 10^2 - 10^5$ μm; computed using the double-Debye expansion with T = 0 — 40 °C.

Distribution

Commandant
U.S. Army Chemical School
ATTN: ATZN-CM-CC (Mr. Barnes)   1
Fort McClellan, AL 36205-5020

NASA Marshal Space Flight Center
Deputy Director
Space Science Laboratory
Atmospheric Sciences Division
ATTN: E501 (Dr. Fichtl)   1
Huntsville, AL 35802

NASA/Marshall Space Flight Center
Atmospheric Sciences Division
ATTN: Code ED-41   1
Huntsville, AL 35812

Deputy Commander
U.S. Army Strategic Defense Command
ATTN: CSSD-SL-L (Dr. Lilly)   1
P.O. Box 1500
Huntsville, AL 35807-3801

Deputy Commander
U.S. Army Missile Command
ATTN: AMSMI-RD-AC-AD (Dr. Peterson)   1
Redstone Arsenal, AL 35898-5242

Commander
U.S. Army Missile Command
ATTN: AMSMI-RD-DE-SE (Mr. Lill, Jr.)   1
Redstone Arsenal, AL 35898-5245

Commander
U.S. Army Missile Command
ATTN: AMSMI-RD-AS-SS (Mr. Anderson)   1
Redstone Arsenal, AL 35898-5253

Commander
U.S. Army Missile Command
ATTN: AMSMI-RD-AS-SS (Mr. B. Williams)   1
Redstone Arsenal, AL 35898-5253

Commander
U.S. Army Missile Command
Redstone Scientific Information Center
ATTN: AMSMI-RD-CS-R/Documents   1
Redstone Arsenal, AL 35898-5241

Commander
U.S. Army Aviation Center
ATTN: ATZQ-D-MA (Mr. Heath)   1
Fort Rucker, AL 36362

Commander
U.S. Army Intelligence Center
  and Fort Huachuca
ATTN: ATSI-CDC-C (Mr. Colanto)   1
Fort Huachuca, AZ 85613-7000

Northrup Corporation
Electronics Systems Division
ATTN: Dr. Tooley   1
2301 West 120th Street, Box 5032
Hawthorne, CA 90251-5032

Commander
Pacific Missile Test Center
  Geophysics Division
ATTN: Code 3250 (Mr. Battalino)   1
Point Mugu, CA 93042-5000

Commander
Code 3331
Naval Weapons Center
ATTN: Dr. Shlanta   1
China Lake, CA 93555

Lockheed Missiles & Space Co., Inc.
Kenneth R. Hardy
ORG/91-01 B/255   1
3251 Hanover Street
Palo Alto, CA 94304-1191

Commander
Naval Ocean Systems Center
ATTN: Code 54 (Dr. Richter)   1
San Diego, CA 92152-5000

Meteorologist in Charge
Kwajalein Missile Range
P.O. Box 67   1
APO San Francisco, CA 96555

U.S. Department of Commerce Center
Mountain Administration
Support Center, Library, R-51
Technical Reports
325 S. Broadway   1
Boulder, CO 80303

Dr. Hans J. Liebe
NTIA/ITS S 3
325 S. Broadway   1
Boulder, CO 80303

NCAR Library Serials
National Center for Atmos Research
P.O. Box 3000   1
Boulder, CO 80307-3000

Headquarters
Department of the Army
ATTN: DAMI-POI   1
Washington, DC 20310-1067

Mil Asst for Env Sci Ofc of
  the Undersecretary of Defense
  for Rsch & Engr/R&AT/E&LS
Pentagon - Room 3D129   1
Washington, DC 20301-3080

Headquarters
Department of the Army
DEAN-RMD/Dr. Gomez   1
Washington, DC 20314

Director
Division of Atmospheric Science
National Science Foundation
ATTN: Dr. Bierly   1
1800 G. Street, N.W.
Washington, DC 20550

Commander
Space & Naval Warfare System Command
ATTN: PMW-145-1G   1
Washington, DC 20362-5100

Director
Naval Research Laboratory
ATTN: Code 4110
  (Mr. Ruhnke)   1
Washington, DC 20375-5000

Commandant
U.S. Army Infantry
ATTN: ATSH-CD-CS-OR (Dr. E. Dutoit)   1
Fort Benning, GA 30905-5090

USAFETAC/DNE   1
Scott AFB, IL 62225

Air Weather Service
Technical Library - FL4414   1
Scott AFB, IL 62225-5458

USAFETAC/DNE
ATTN: Mr. Glauber   1
Scott AFB, IL 62225-5008

Headquarters
AWS/DOO   1
Scott AFB, IL 62225-5008

Commander
U.S. Army Combined Arms Combat
ATTN: ATZL-CAW   1
Fort Leavenworth, KS 66027-5300

Commander
U.S. Army Space Institute
ATTN: ATZI-SI   1
Fort Leavenworth, KS 66027-5300

Commander
U.S. Army Space Institute
ATTN: ATZL-SI-D   1
Fort Leavenworth, KS 66027-7300

Commander
Phillips Lab
ATTN: PL/LYP (Mr. Chisholm)   1
Hanscom AFB, MA 01731-5000

Director
Atmospheric Sciences Division
Geophysics Directorate
Phillips Lab
ATTN: Dr. McClatchey   1
Hanscom AFB, MA 01731-5000

Raytheon Company
Dr. Sonnenschein
Equipment Division
528 Boston Post Road   1
Sudbury, MA 01776
Mail Stop 1K9

Director
U.S. Army Materiel Systems Analysis Activity
ATTN: AMXSY-CR (Mr. Marchetti)   1
Aberdeen Proving Ground, MD 21005-5071

Director
U.S. Army Materiel Systems Analysis Activity
ATTN: AMXSY-MP (Mr. Cohen)   1
Aberdeen Proving Ground, MD 21005-5071

Director
U.S. Army Materiel Systems Analysis Activity
ATTN: AMXSY-AT (Mr. Campbell)   1
Aberdeen Proving Ground, MD 21005-5071

Director
U.S. Army Materiel Systems
  Analysis Activity
ATTN: AMXSY-CS (Mr. Bradley)   1
Aberdeen Proving Ground, MD 21005-5071

Director
ARL Chemical Biology
Nuclear Effects Division
ATTN: AMSRL-SL-CO   1
Aberdeen Proving Ground, MD 21010-5423

Army Research Laboratory
ATTN: AMSRL-D   1
2800 Powder Mill Road
Adelphi, MD 20783-1145

Army Research Laboratory
ATTN: AMSRL-OP-SD-TP   1
Technical Publishing
2800 Powder Mill Road
Adelphi, MD 20783-1145

Army Research Laboratory
ATTN: AMSRL-OP-CI-SD-TL   1
2800 Powder Mill Road
Adelphi, MD 20783-1145

Army Research laboratory
ATTN: AMSRL-SS-SH   1
  (Dr. Sztankay)
2800 Powder Mill Road
Adelphi, MD 20783-1145

U.S. Army Space Technology
  and Research Office
ATTN: Ms. Brathwaite   1
5321 Riggs Road
Gaithersburg, MD 20882

National Security Agency
ATTN: W21 (Dr. Longbothum)   1
9800 Savage Road
Fort George G. Meade, MD 20755-6000

OIC-NAVSWC
Technical Library (Code E-232)   1
Silver Springs, MD 20903-5000

Commander
U.S. Army Research office
ATTN: DRXRO-GS (Dr. Flood)   1
P.O. Box 12211
Research Triangle Park, NC 27009

Dr. Jerry Davis
North Carolina State University
Department of Marine, Earth, and
  Atmospheric Sciences   1
P.O. Box 8208
Raleigh, NC 27650-8208

Commander
U.S. Army CECRL
ATTN: CECRL-RG (Dr. Boyne)   1
Hanover, NH 03755-1290

Commanding Officer
U.S. Army ARDEC
ATTN: SMCAR-IMI-I, Bldg 59   1
Dover, NJ 07806-5000

Commander
U.S. Army Satellite Comm Agency
ATTN: DRCPM-SC-3   1
Fort Monmouth, NJ 07703-5303

Commander
U.S. Army Communications-Electronics
  Center for EW/RSTA
ATTN: AMSEL-EW-MD   1
Fort Monmouth, NJ 07703-5303

Commander
U.S. Army Communications-Electronics
  Center for EW/RSTA
ATTN: AMSEL-EW-D   1
Fort Monmouth, NJ 07703-5303

Commander
U.S. Army Communications-Electronics
 Center for EW/RSTA
ATTN: AMSEL-RD-EW-SP   1
Fort Monmouth, NJ 07703-5206

Commander
Department of the Air Force
OL/A 2d Weather Squadron (MAC)   1
Holloman AFB, NM 88330-5000

PL/WE   1
Kirtland AFB, NM 87118-6008

Director
U.S. Army TRADOC Analysis Center
ATTN: ATRC-WSS-R   1
White Sands Missile Range, NM 88002-5502

Director
U.S. Army White Sands Missile Range
Technical Library Branch
ATTN: STEWS-IM-IT   3
White Sands Missile Range, NM 88002

Army Research Laboratory
ATTN: AMSRL-BE (Mr. Veazy)   1
Battlefield Environment Directorate
White Sands Missile Range, NM 88002-5501

Army Research Laboratory
ATTN: AMSRL-BE-A (Mr. Rubio)   1
Battlefield Environment Directorate
White Sands Missile Range, NM 88002-5501

Army Research Laboratory
ATTN: AMSRL-BE-M (Dr. Niles)   1
Battlefield Environment Directorate
White Sands Missile Range, NM 88002-5501

Army Research Laboratory
ATTN: AMSRL-BE-W (Dr. Seagraves)   1
Battlefield Environment Directorate
White Sands Missile Range, NM 88002-5501

68

USAF Rome Laboratory Technical
Library, FL2810   1
Corridor W, STE 262, RL/SUL
26 Electronics Parkway, Bldg 106
Griffiss AFB, NY 13441-4514

AFMC/DOW   1
Wright-Patterson AFB, OH 03340-5000

Commandant
U.S. Army Field Artillery School
ATTN: ATSF-TSM-TA (Mr. Taylor)   1
Fort Sill, OK 73503-5600

Commander
U.S. Army Field Artillery School
ATTN: ATSF-F-FD (Mr. Gullion)   1
Fort Sill, OK 73503-5600

Commander
Naval Air Development Center
ATTN: Al Salik (Code 5012)   1
Warminister, PA 18974

Commander
U.S. Army Dugway Proving Ground
ATTN: STEDP-MT-M (Mr. Bowers)   1
Dugway, UT 84022-5000

Commander
U.S. Army Dugway Proving Ground
ATTN: STEDP-MT-DA-L   1
Dugway, UT 84022-5000

Defense Technical Information Center
ATTN: DTIC-OCP   2
Cameron Station
Alexandria, VA 22314-6145

Commander
U.S. Army OEC
ATTN: CSTE-EFS   1
Park Center IV
4501 Ford Ave
Alexandria, VA 22302-1458

Commanding Officer
U.S. Army Foreign Science & Technology Center
ATTN: CM   1
220 7th Street, NE
Charlottesville, VA 22901-5396

Naval Surface Weapons Center
Code G63   1
Dahlgren, VA 22448-5000

Commander and Director
U.S. Army Corps of Engineers
Engineer Topographics Laboratory
ATTN: ETL-GS-LB   1
Fort Belvoir, VA 22060

U.S. Army Topo Engineering Center
ATTN: CETEC-ZC   1
Fort Belvoir, VA 22060-5546

Commander
USATRADOC
ATTN: ATCD-FA   1
Fort Monroe, VA 23651-5170

TAC/DOWP   1
Langley AFB, VA 23665-5524

Commander
Logistics Center
ATTN: ATCL-CE   1
Fort Lee, VA 23801-6000

Science and Technology
101 Research Drive   1
Hampton, VA 23666-1340

Commander
U.S. Army Nuclear and Chemical Agency
ATTN: MONA-ZB, Bldg 2073   1
Springfield, VA 22150-3198

Record Copy   3

Total   89

70